FSEC-NSG-217-75/50
ERDA-SNS-3063-7

NUCLEAR HEAT SOURCES FOR CRYOGENIC REFRIGERATOR APPLICATIONS

Prepared for

USAF SPACE & MISSILE SYSTEM ORGANIZATION

Under

ENERGY RESEARCH &
DEVELOPMENT ADMINISTRATION
CONTRACT NO. AT (49-15) - 3063, TASK 6

6 JUNE 1975

FAIRCHILD
SPACE & ELECTRONICS COMPANY
Germantown, Maryland 20767

DISCLAIMER

FSEC-NSG-217-75/50
ERDA-SNS-3063-7

NUCLEAR HEAT SOURCES FOR CRYOGENIC REFRIGERATOR APPLICATIONS

Prepared for

USAF SPACE & MISSILE SYSTEM ORGANIZATION

Under

ENERGY RESEARCH &
DEVELOPMENT ADMINISTRATION
CONTRACT NO. AT (49-15) - 3063, TASK 6

6 JUNE 1975

Prepared by:
BERNARD RAAB

ALFRED SCHOCK
WILLIAM G. KING
THOMAS KLINE
FRANK A. RUSSO,
TELEDYNE ENERGY SYSTEMS

1.0 INTRODUCTION & SUMMARY

1.1 BACKGROUND

Spaceborne cryogenic refrigerators, e.g. for cooling infrared detectors, require thermal inputs on the order of 1000 watts. These can be provided in a number of ways, such as solar-electric, solar-thermal, and nuclear, to name the most obvious candidates. Those options were considered in an earlier study[1], which concluded that the solar-electric approach was preferable, mainly due to state-of-the-art readiness. However, the only nuclear option considered was the reactor-thermoelectric system, although an isotope heat source appears to be a much better choice for the desired thermal power of approximately 1000 watts.

Plutonium-238 heat sources in the range of 500 to 1500 watts(t) have been space-borne since 1963. Starting in 1969, 1500-watt heat sources were used to power the SNAP-27 generator for the Apollo Lunar Surface Experiments Package (ALSEP). The current-generation heat source, described in Appendix A,is designed for the Multi-Hundred-Watt (MHW) generator[2] scheduled to be launched in 1975, and produces 2400 watts(t). Such heat sources typically weigh less than 50 pounds in the power ranges noted, whereas the minimum-weight nuclear reactor system will be in the range of 700 to 1000 pounds, including shielding. Moreover, the radiation emitted by a plutonium-238 heat source, without shielding, is orders-of-magnitude lower than that from an equal-power reactor with a several-hundred-pound shadow shield (see Appendix B for Pu-238 data). Under the circumstances, the choice of radioisotope power in preference to reactor power for the cryo-refrigerator thermal requirement hardly needs belaboring.

1.2 NUCLEAR AND SOLAR-ELECTRIC COMPARISONS

The choice between radioisotope-thermal power and solar-electric-thermal power is not quite so obvious, and should properly be made in the systems context. However, certain general comparisons can be made on a

first-order basis. These are summarized in Table 1 for a nominal 1000 watt(t) requirement.

The major advantages of the radioisotope approach are low weight and size, permitting weight savings of several hundred pounds per spacecraft (depending on power requirements), as well as lower cost for equal hardness levels. Relative to a fully-hardened roll-up solar array, the cost of an isotope heat source per thermal watt can be substantially lower, as indicated in Table 1. Moreover, 50 to 70% of this cost (that of a fuel material itself) is borne by an intra-governmental transfer of funds and is not subjected to contractor and system-level burdens, as are solar-array costs.

[An all-nuclear spacecraft, containing nuclear-electric as well as thermal power, would offer the additional advantage of eliminating all sun-pointing requirements. This can be a potentially significant advantage to observation satellites with other spatial pointing requirements, since it may allow the elimination of rotating joints and/or gimbaled sensors. Approaches to the design of all nuclear Hysat satellites are described in a separate report, where they are compared with the all-solar or hybrid (solar-electric, nuclear thermal) approaches studied by the Hysat contractors.]

A disadvantage of radioisotope thermal systems is their constant heat output, which requires special means for heat removal on the ground and through the launch phase. Since temporary space-shutdown of the refrigerator for an indefinite duration has been postulated, a reversible method for switching the heat flow path directly to space during these shutdown periods is required.

Concerning nuclear safety, each radioisotope heat source is designed and qualified for safety under all credible accident conditions. This is the sole responsibility of the Energy Research & Development Administration (ERDA).

TABLE I.

Comparative Characteristics; 1000 watt(t) Requirement

Characteristic	Solar-Electric	Radioisotope
Current state-of-the-art	Roll-up arrays; Ni-Cd batteries	MHW heat source modules (100 w each)
Weight range, lb	200-400 (incl. batteries)‡*	30-50
Size range	Several ft^3 stowed 80-150 ft^2 deployed	$\sim\frac{1}{2}$ ft^3
Cost range, k$	1000 - 2000 ‡	700 - 1000
Orientation required	sun-pointed	none
Advantages	"standard" approach; control system developed: adaptable to Vuilleumier and Rotary Reciprocating Refrigerators	low-weight; eliminates batteries or thermal storage; adaptable to VM and R^3 (with thermal compressor)
Disadvantages	large extended area; requires deployment, sun orientation; high visibility	Requires: special ground handling and cooling; thermal-control mechanism for space shutdown

‡ Depending on hardness requirements

* Weight breakdown in Phase III Report, "Fifth Semiannual Hardened Solar Power System Presentation", Hughes Aircraft Co., 46497-1, AFAPL Contract F 33615-71-C-1792, shows a weight of 375 lb/kw for solar arrays, orientation, regulation and control, harness, battery and charge controller.

All design and supporting data are subject to pre-launch review and user-agency approval. The Air Force Weapons Laboratory has been designated as the lead DoD center for safety review of radioisotope heat sources, and the entire review procedure is by now well established. Although this procedure may differ in level of detail, it is not different in principle from the launch safety review normally required of space hardware of any kind.

Finally, approval of the National Security Council is required, because of the foreign policy implications of orbiting nuclear material. However, this has never been denied once recommended by the cognizant agency. Approval for purely scientific as well as national-security-related missions has been granted routinely.

1.3 SUMMARY

The external interface requirements, together with the internal thermal and safety requirements of the heat sources, provided the major design constraints to the heat source system described here. The various requirements appear to be amenable to rather simple and elegant solutions, which allow the use of existing refrigerator designs without alteration.

Section 2 of the report describes a possible state-of-the-art heat source design approach, based on the use of MHW fuel sphere assemblies (FSA's). The heat source contains proven safety provisions for all credible accident conditions. A simple reversible thermal switching method, operated on command, is also described. The system is fail-safe, i.e., in the event of simultaneous failure of the refrigerator and thermal switch, an emergency heat dump will reduce the fuel temperature to a relatively low value.

The recommended spacecraft thermal interface unit, which also provides the thermal interface with the space-shuttle orbiter or with a disposable booster, is described in Section 3.

Special ground-handling methods are required for radioisotope fuels, but these have not proved to be an obstacle to their use in past missions. Experience in handling and launching radioisotope fuel has now been achieved

at both Eastern and Western Test Ranges. The general gound-handling and launch methods which will apply to the nuclear heat sources are described in Section 4.

Finally, an alternative heat source design, based on more advanced fuel element concepts and thermal control schemes, is presented in Section 5. These concepts result in a lighter and perhaps lower cost heat source. The thermal interface system described in Section 3 and the ground handling sequence discussed in Section 4 would be applicable to either heat source design.

2.0 STATE-OF-THE-ART HEAT SOURCE DESIGN

2.1 REFRIGERATOR REQUIREMENT

The heat source design shown here is based on satisfying the thermal requirements of the existing Hughes Hi-Cap Vuilleumier (VM) refrigerator.[3] However, these designs can be adapted with minor modifications to other refrigerators, including the Rotary Reciprocating machines now in development. To be operated thermally, the latter would be provided with thermal compressors.[4] A basic design groundrule was that no modification of the VM machine would be required.

The electrically heated VM unit is depicted in Figure 1, and a more detailed view of one of its two hot-end assemblies is presented in Figure 2. The isotope heat source package replaces the electrical heater and insulation assembly which surround the hot cylinder. If desired, the isotope heat source can be installed after the VM unit has first been checked out with electrical heaters.

The refrigerator can be operated over a wide range of heat inputs, depending on the cooling load, varying from perhaps 500 to 1500 watts(t) per cylinder. Nominal hot cylinder external wall temperature is 1275°F (690°C).

Figure 2 also shows the coolant passages through which flows the low temperature refrigerator coolant. This coolant carries the entire compressor heat input plus the cooling load to a space radiator which operates in the range of 70-to-100°F.

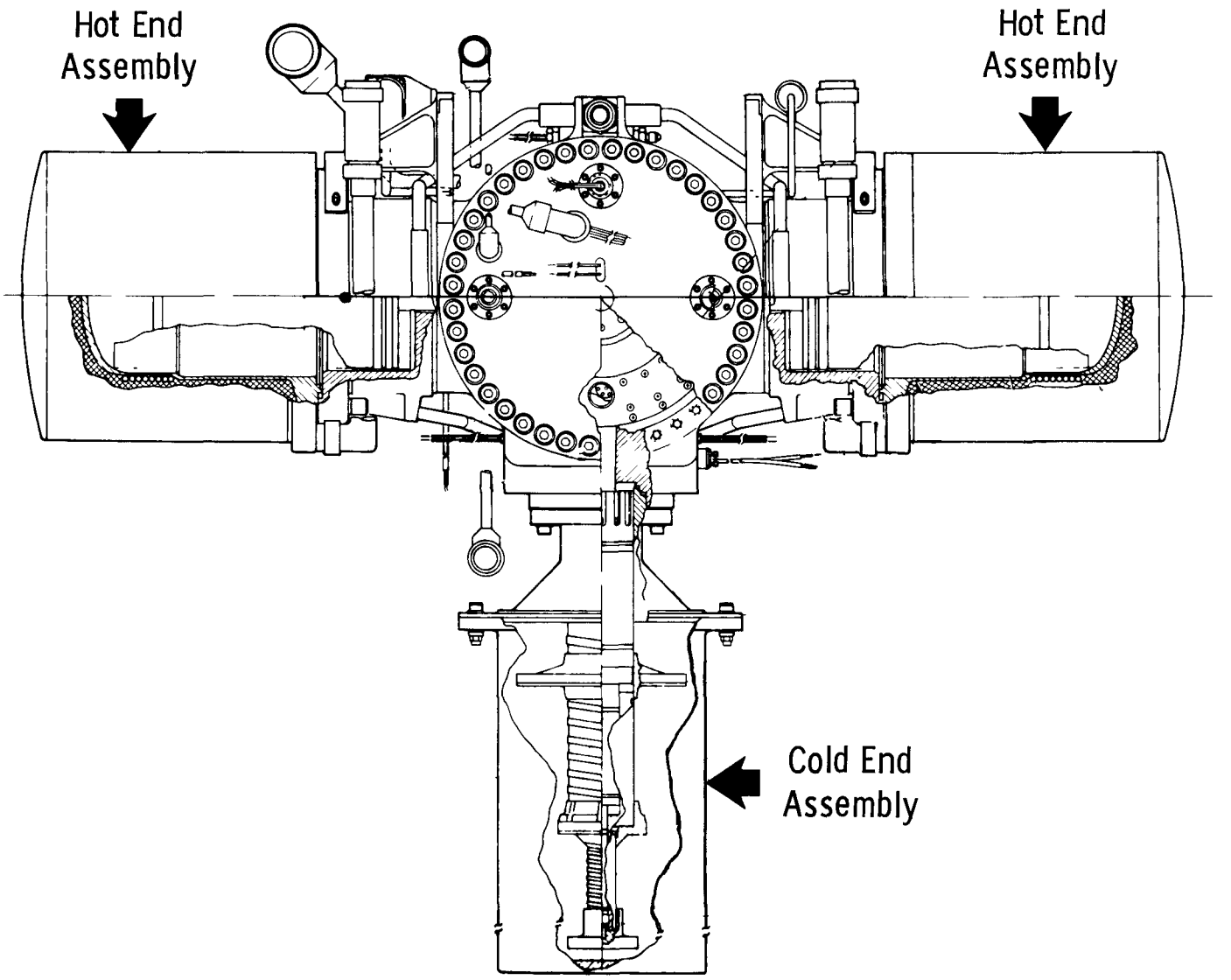

Figure 1

VM REFRIGERATOR

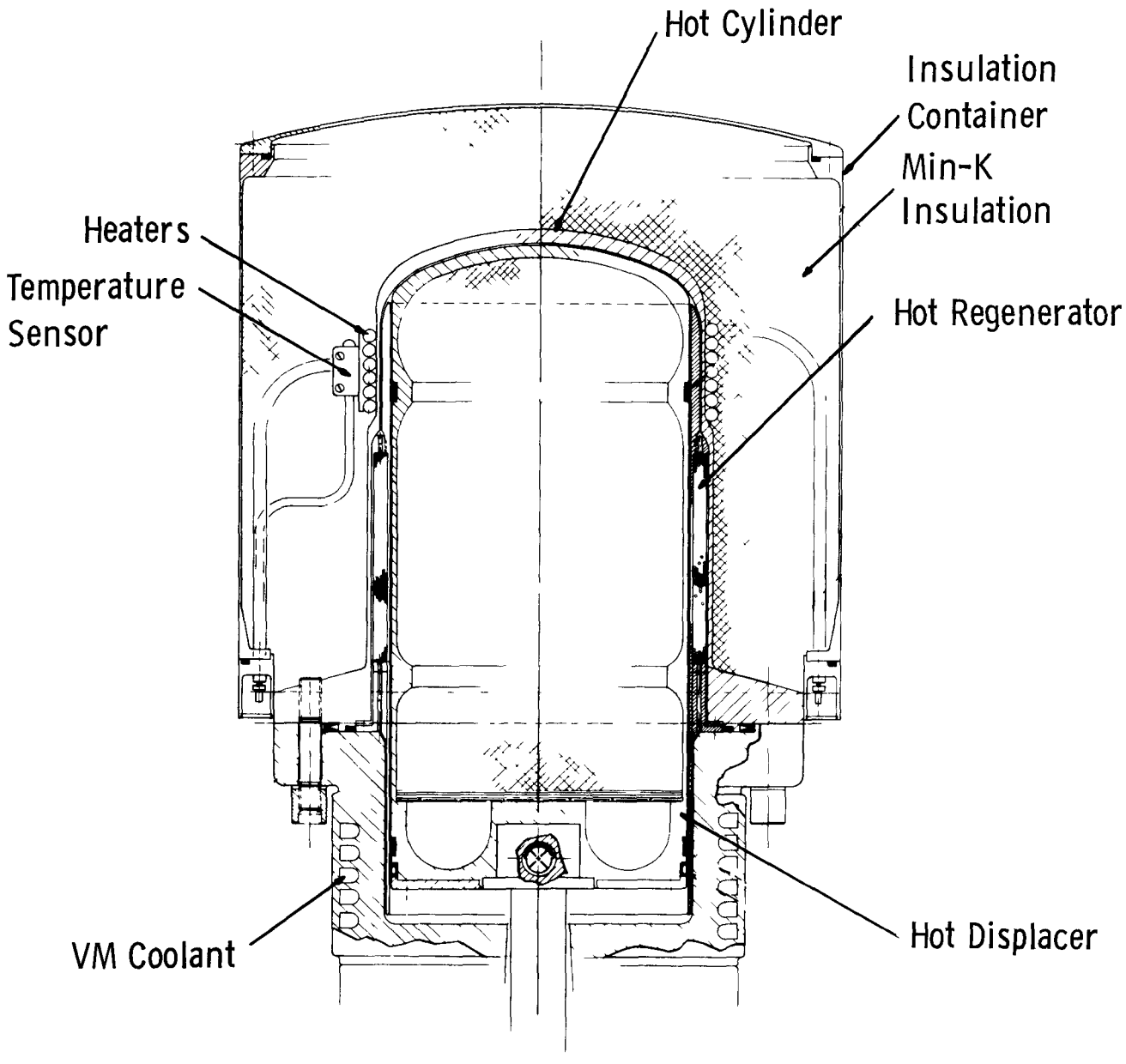

Figure 2 VM REFRIGERATOR HOT-END ASSEMBLY

2.2 DESIGN APPROACH

Safety considerations have a strong influence on the design of isotope heat sources, which must be certified by ERDA to have an adequate complement of built-in safety provisions to ensure that the probability of fuel release in any credible accident mode or combination of accidents is acceptably low. Such accidents include booster detonation, shrapnel dispersion, solid-fuel fire immersion, aerodynamic heating during reentry, impact on granite, post-impact burial and oxidation. All these problems have been addressed and solved on previous isotope-powered flight programs.

An isotope heat source design for the cooler application can be based either on existing fuel elements, which have already been developed and qualified, or on new designs, using the lessons from previous development programs to guide the solution of the various safety and operational requirements. The latter approach would result in a lighter and possibly lower-cost heat source, since the design could be optimized for the specific mission. The former approach, i.e., the use of proven fuel element designs, minimizes schedule risk for near-term applications. The ultimate choice will depend on the relative importance of these competing factors in a given program.

The design described in this section is based on existing fuel elements; i.e., the fuel sphere assembly (FSA) developed for the multi-hundred watt (MHW) thermoelectric generator, scheduled for first flight in late 1975. (See Appendix A). The FSA design was qualified in a lengthy series of safety analyses and tests. Each FSA consists of 1.6"-diameter PuO_2 sphere, encapsulated in a 0.020"-thick vented iridium shell, enclosed in a 0.45"-thick impact absorption shell made of a (Thornel) carbon-carbon composite. Each FSA has an initial thermal power of 100 watts, which diminishes at the rate of 0.8% per year as the result of fuel decay.

Since the exact heat input required by the refrigerator is somewhat variable, the design shown is based on a nominal number of ten FSAs (1000 watts) for each of the two hot-end assemblies. Higher or lower power levels, within reason, could be accommodated by relatively simple design modifications.

The FSAs have demonstrated adequate high-temperature physical and chemical stability, and resistance to vent plugging. The operating temperature of the iridium capsule and helium vent in the reference heat source is calculated to be 1720°F, compared to their operating temperature of 2435°F in the MHW generator. This enhances material stability and vent integrity. At the predicted heat source impact velocity (165 ft/sec at sea level) they also have more than adequate impact resistance, without any additional impact absorber.

Their resistance to launch pad accidents and the reentry heat pulse, however, depends not only on the FSA's themselves, but also on the protection provided by the package in which they are contained. In general, that package consists of a graphite ablator, thermal insulation to prevent excessive iridium temperatures during a solid-fuel fire and during reentry, and an outer metallic can to protect the other components from shrapnel damage.

The heat source design can be based on an individual package for each fuel element, for groups of fuel elements, or on a single package for all ten FSAs. The design described in this section uses the single-package approach, as shown in Figure 3.

The ten fuel sphere assemblies nest in a graphite reentry body, 4.4 inches high and 11.8 inches in outer diameter. The body is split, to permit FSA insertion, and its two halves are held together by a graphite snap ring. This is the same locking arrangement as that used in the MHW heat source for the Mariner-Jupiter/Saturn (MJS-77) mission. The reentry body is Pyrocarb, which is a composite formed by graphite-bonding stacked layers of graphite cloth. It has excellent thermal stress resistance, is a good thermal insulator in the transplanar direction (to reduce the peak FSA temperature during reentry or in a solid-fuel fire), and provides additional impact protection.

The reentry body is contained in an inner and outer can of superalloy, sealed by an O-ring closure. (If desired, an all-welded design could be substituted, but this would require making the final weld in a hot cell, after fuel insertion.) The inner can has a cavity of 4.57-inch diameter, which fits over

Figure 3.

1000 WATT ISOTOPE HEAT SOURCE FOR VUILLEUMIER COOLER

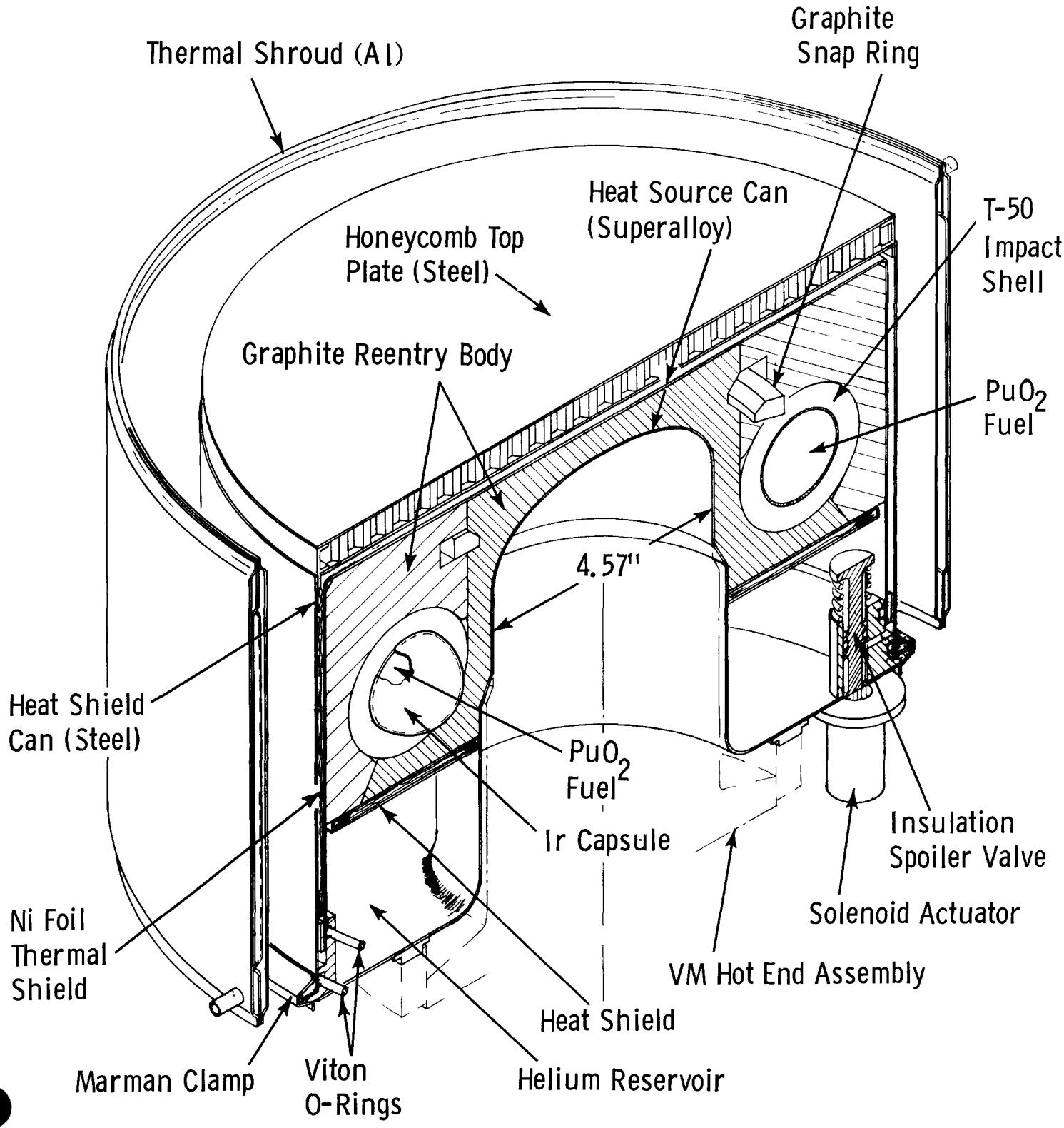

the outside of the 1275°F hot cylinder of the VM unit. The sides and end face of the outer can are surrounded by multiple layers of nickel foils, which are coated with small spheres of zirconia to minimize thermal conduction between them. The foils are contained in an outside can of steel, whose end face is stiffened by an integral honeycomb structure.

2.3 THERMAL CONTROL

Special thermal control problems arise because isotope heat sources, unlike electrical heaters, cannot be turned off. Therefore, a reliable method must be provided for removing the isotope decay heat during the non-operating period of the refrigerator. That method must be reversible, to permit resumption of refrigerator operation, and must not add any significant heat losses when the unit is operating. Moreover, the entire system must be fail-safe, in the sense that even when all active control systems fail, passive systems will keep the fuel elements cool enough to prevent fuel release.

These thermal requirements are satisfied by the nickel foil layers which surround the outside of the heat source. During normal operation, the space between the foils is evacuated (i.e., open to space) and the foil assembly acts as a very effective thermal radiation shield. When the refrigerator is to be shut down, the heat source is kept at a benign temperature by admitting helium into the interfoil space. As little as ten torr of helium will effectively spoil the thermal insulation, allowing heat rejection from the heat source's outer surface. This thermal switching process is reversible, since the interfoil space can be repeatedly filled and vented to space. Thus the refrigerator can be turned on and off, as desired. As will be explained, the helium supply is continually replenished by the helium generation resulting from the fuel's alpha decay.

The fail-safe emergency cooling feature is achieved by making the insulating foil out of nickel or ferrous alloy rather than refractory metal. Thus, in case of a serious malfunction, the insulation package would melt before the fuel elements reach excessive temperatures. A NASA-LeRC sponsored program to develop an isotope heat source for a Brayton-cycle

generator has successfully demonstrated this emergency cooling system on a small scale, and is proceeding to a full-scale test.[5]

Figure 3 also shows the toroidal helium reservoir, which is separated from the reentry package by a multi-foil heat shield. Since the reservoir is in communication with the vented fuel sphere assemblies, there is a constant supply of fresh helium from alpha decay. Excessive pressure buildup is prevented by helium leakage through the Viton O-rings which joins the inner and outer heat source cans. Leak rates of such O-rings as a function of temperature have been extensively measured in previous isotope power programs, and are quite predictable. For the present design, they will be dimensioned to yield a reservoir equilibrium pressure of approximately one atmosphere. Note that the interior volume of the heat source is always flooded with helium. This promotes heat transfer across interface gaps.

Finally, Figure 3 shows the solenoid-actuated insulation spoiler valve, which is used to switch the multi-foil assembly from its operational (low-conductance) to its non-operational (high-conductance) mode. The valve body is integral with the closure ring which seals both the heat source can and the heat shield can. With the solenoid actuator passive as shown, the spring raises the valve stem, which seals the reservoir and vents the interfoil volume to space vacuum. When the refrigerator is to be shut off, the solenoid is actuated, which lowers the valve stem to connect the helium reservoir to the interfoil space. Reversing the cycle vents the helium from the interfoil volume to space, permitting resumption of refrigerator operation. Since the interfoil volume is but 2 to 3% of the reservoir volume, only a small fraction of the helium supply is lost on each on-off cycle. Thus, even if there were no helium replenishment from alpha-decay, more than 100 on-off cycles would be possible before the helium pressure drops below the pressure (10 torr) required to spoil the insulation. Note that even if the spoiler valve were to leak or the solenoid actuator were to fail, the foil insulation would still be vented to space and the refrigerator could continue to function.

The weight breakdown of the 1000-watt heat source assembly (HSA) is shown in Table 2. The heaviest component is seen to be the 17.8 lb. graphite reentry body, which has been rather conservatively designed and could probably be lightened. The ten FSAs have a combined weight of 9.8 lbs., and the total heat source weight is almost 42 lbs.

Table 2.

Heat Source Assembly Weight Summary (lbs.)

Item	1000 Watt(t)
Fuel Sphere Assemblies	9.8
Graphite Reentry Body	17.8
Inner Heat Source Can	2.3
Outer Heat Source Can	2.9
Foil Thermal Shield	1.3
Heat Shield Can (inc. honeycomb)	4.2
Closure Ring	1.4
Attachment Ring	0.5
Miscellaneous	1.6
	41.8

3.0 SPACECRAFT THERMAL INTERFACES

The spacecraft thermal interface requirements pertain not only to normal operation, but also to ground assembly, launch sequence, including extended hold periods, and to in-orbit shutdown periods when the refrigerator is not operating. During non-operational periods, the insulation will be spoiled, thereby dumping the HSA heat to the ambient environment.

When the refrigerator is shut down in orbit, the heat passing through the spoiled insulation must be radiated to space. This could be done directly, by requiring that the heat sources be located external to the spacecraft and the refrigerator radiator. However, this undesirable design constraint can be avoided by using the existing radiator of the VM refrigerator to reject the waste heat during the non-operational as well as the operational periods.

To accomplish this, each heat source is surrounded by a small thermal shroud (see Figure 3), through which the refrigerator coolant passes before going to the existing space radiator (as shown schematically in Figure 4). During normal operation, practically no heat passes through the multi-foil insulation, and the thermal shroud has virtually no effect on the coolant. When the refrigerator is off, the coolant still receives essentially the same amount of heat as during normal operation; only instead of receiving it via the operating refrigerator, it receives it directly from the heat source, through the spoiled multi-foil insulation. Thus, the radiator always operates at the same temperature of less than 100°F. It can therefore be used to surround the spacecraft payload with a fixed low-temperature envelope, regardless of external or load variations.

Since the coolant flow path is always the same, and always operating, there is no need for valving, venting, start-ups, or shut-downs. The low-temperature cooling system should therefore have a high reliability, which could be further enhanced by addition of a redundant coolant pump.

Figure 5 shows temperatures at various locations within the heat source assembly during both normal operation (Fig. 5a) and during refrigerator shut-down with spoiled insulation (Fig. 5b). These calculations and various other cases are reported in Appendix C.

The above system can be easily modified to also satisfy the thermal requirements before and during launch, and the post-launch requirement before the shuttle bays are opened. This can be done by providing the thermal shroud with a second, water-cooled loop, which is connected to the ground-support or launch-vehicle auxilliary cooling system. Thus, the thermal-shroud would act as a heat-source heat exchanger. In the shuttle, the auxilliary cooling loop would transfer heat to the cargo bay heat rejection system, which will be available for heat-dissipating payloads.

The thermal shroud is in the form of an aluminum cylinder, with a 16-inch I.D., and an 8.5-inch height. It weighs approximately 5 lbs. With

Figure 4

SPACECRAFT THERMAL INTERFACES

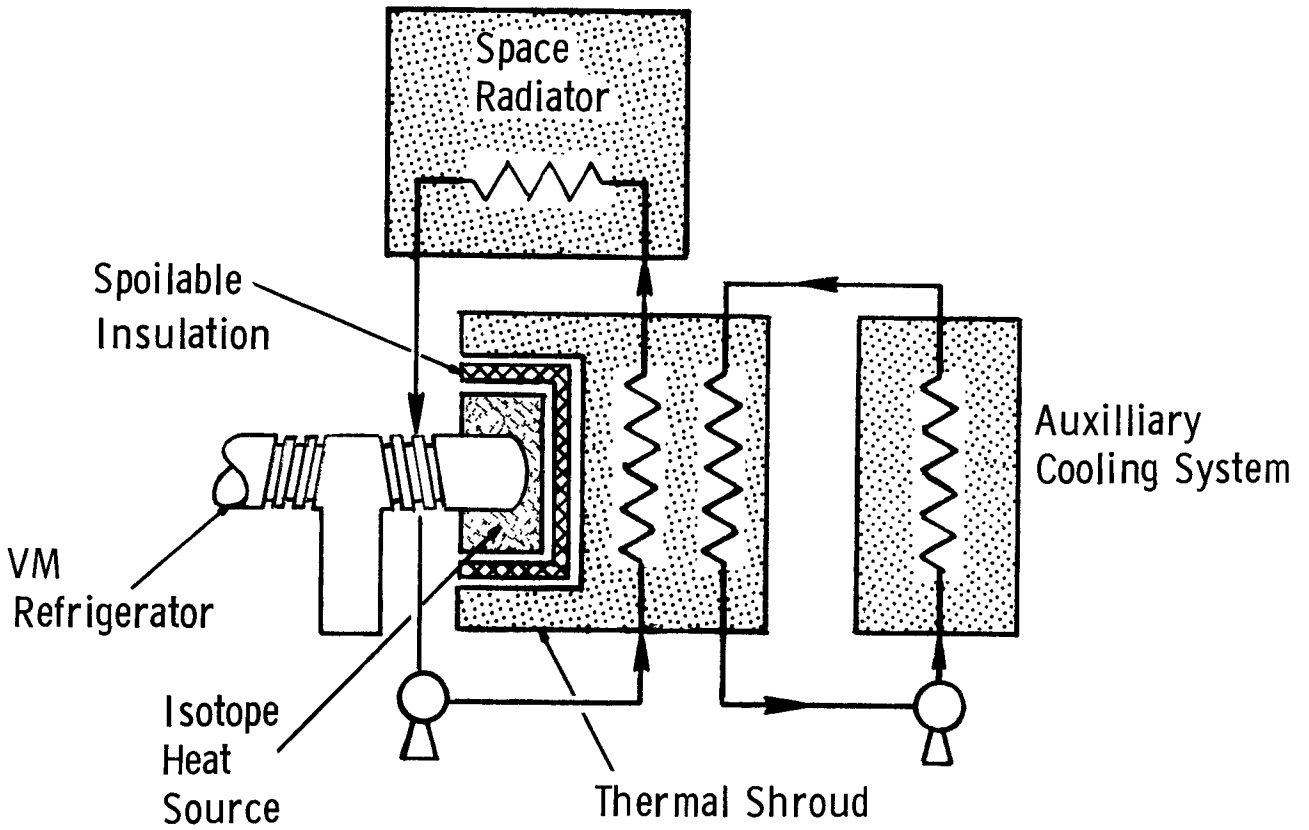

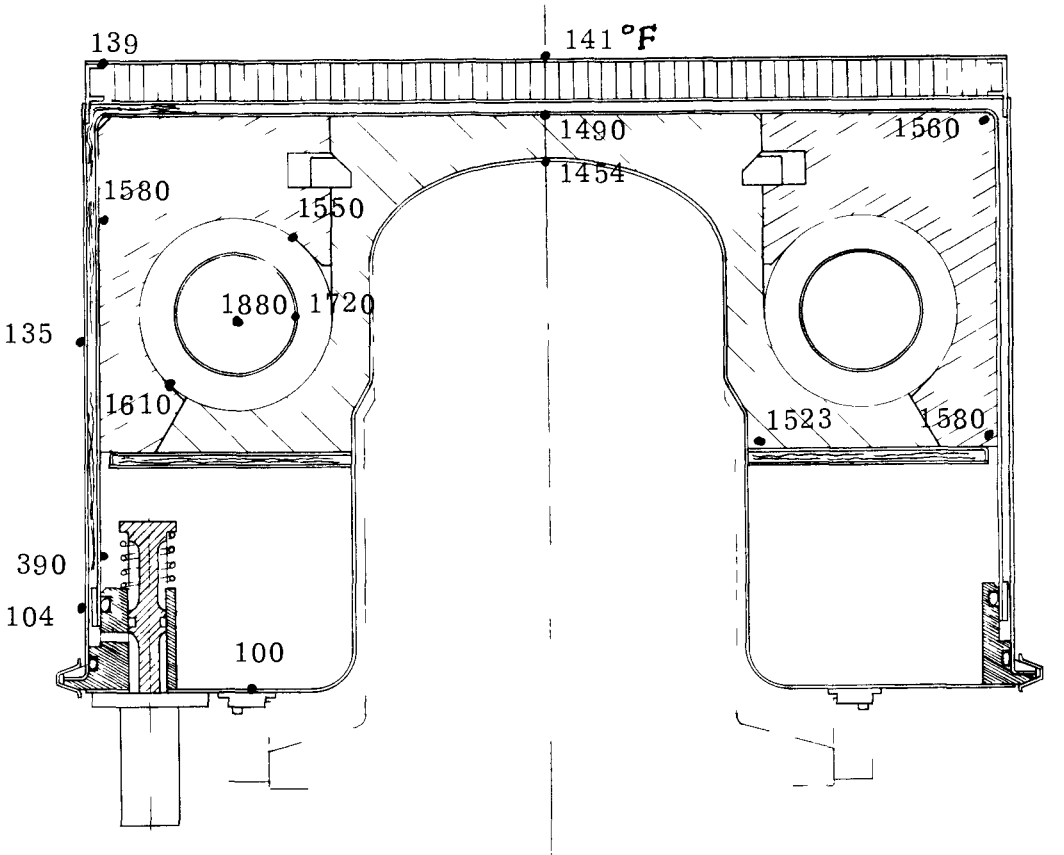

Figure 5A
Normal Operation

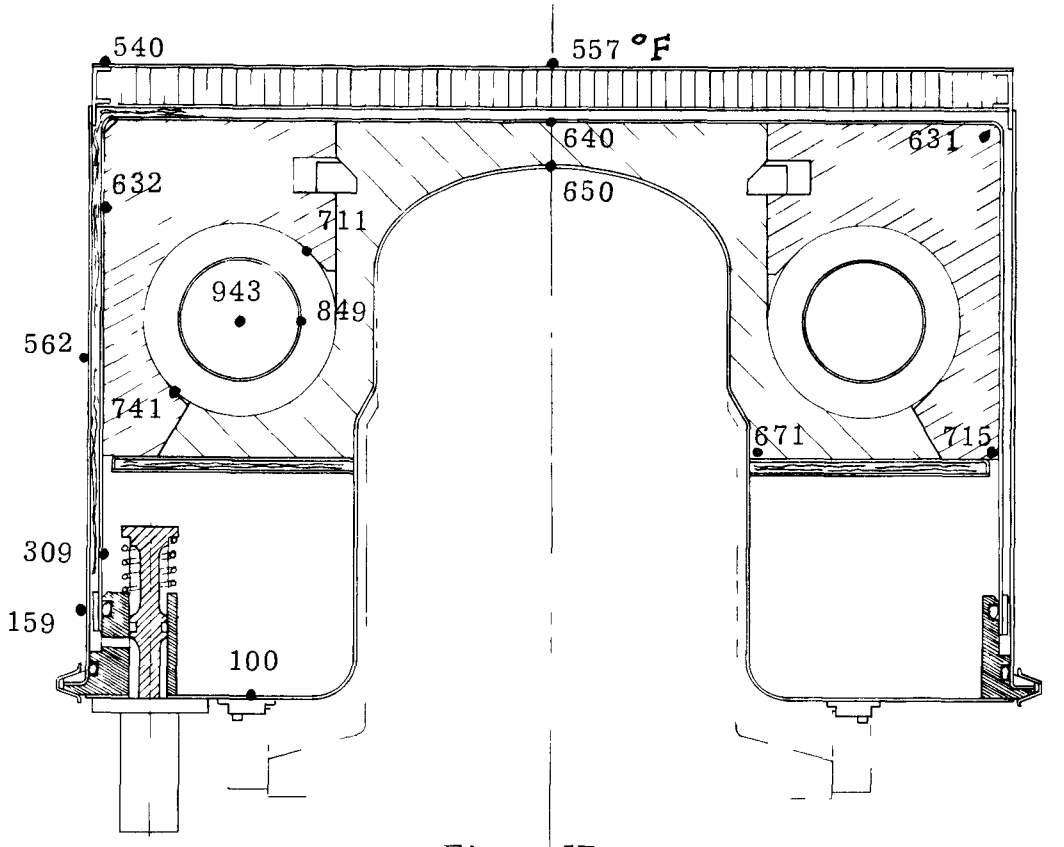

Figure 5B
Refrigerator Shutdown Mode; Insulation Spoiled

coolant flowing in the shroud, the shroud temperature is maintained at $\sim 100^{o}F$. After a period of time in space the coolant pumps will inevitably fail and the shroud temperature will rise to approximately $450^{o}F$. However, the heat source temperature will rise only to approximately $750^{o}F$ on the exterior surface. The emergency heat dump condition leads to similarly low heat source temperature (see Appendix C). Design parameters of the thermal shroud are given in Appendix D.

4.0 GROUND HANDLING SEQUENCE AND REQUIREMENTS

Ground handling of the HSA is governed by two major considerations: radiological safety and thermal control. Personnel access can proceed with essentially no restrictions beyond a few meters of an unshielded Pu-238 heat source. At one meter, a worker can experience approximately 200 hours of exposure per calendar quarter without exceeding the occupational dose limit. Access to the surface of the heat source for several hours per calendar quarter is also permissible, but will most likely be limited as much by thermal as by nuclear considerations. Typically the HSA will be handled on the ground by long-handled tools and by portable lifts.

A generalized ground-handling sequence for the radioisotope heat sources is shown in Figure 6. Final assembly of the HSA will be performed at the facility of the fuel fabricator, using the components and assembly procedure developed by the heat source contractor (See block 1.0 in Figure 6).

Following final radiological check-out for fuel integrity and container cleanliness, a final test of the helium thermal control apparatus will be conducted (2.0). The system will then be sealed with a full helium charge (nominally 1 atmosphere) within the foils and HSA. Heat source cooling will be accomplished by inserting the HSA into a finned structure which clamps securely to the outer case of the HSA. The HSA with its protective structure is then loaded within the DOT-approved shipping container (Figure 7) and shipped to the launch site via dedicated truck with security escort (3.0).

Figure 6.

HEAT SOURCE GROUND FLOW

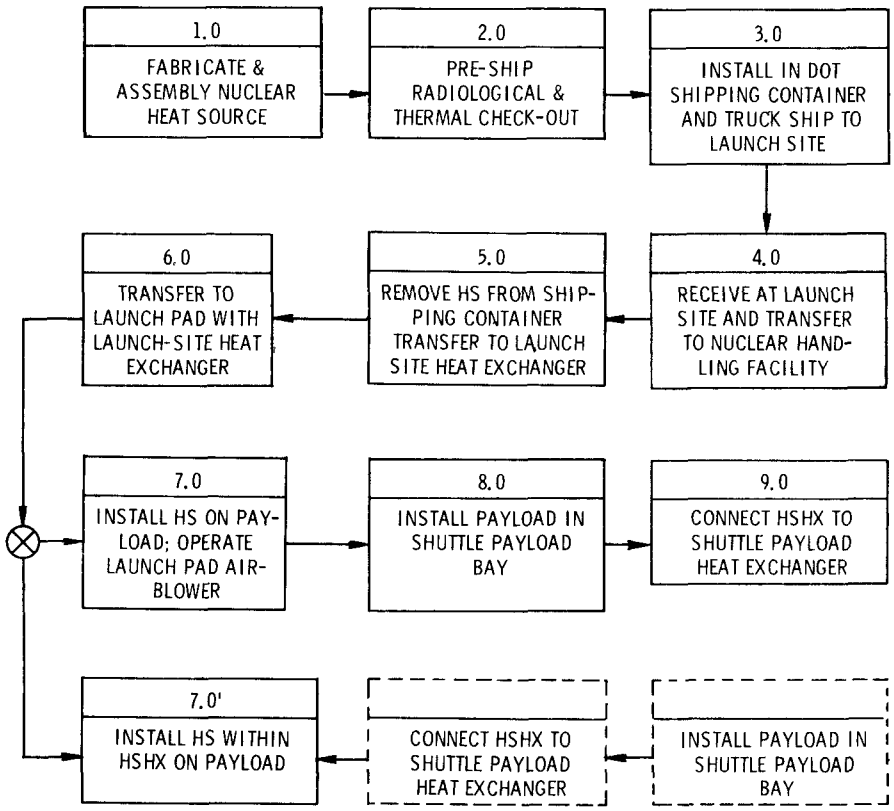

Figure 7.

HEAT SOURCE ASSEMBLY SHIPPING CONTAINER

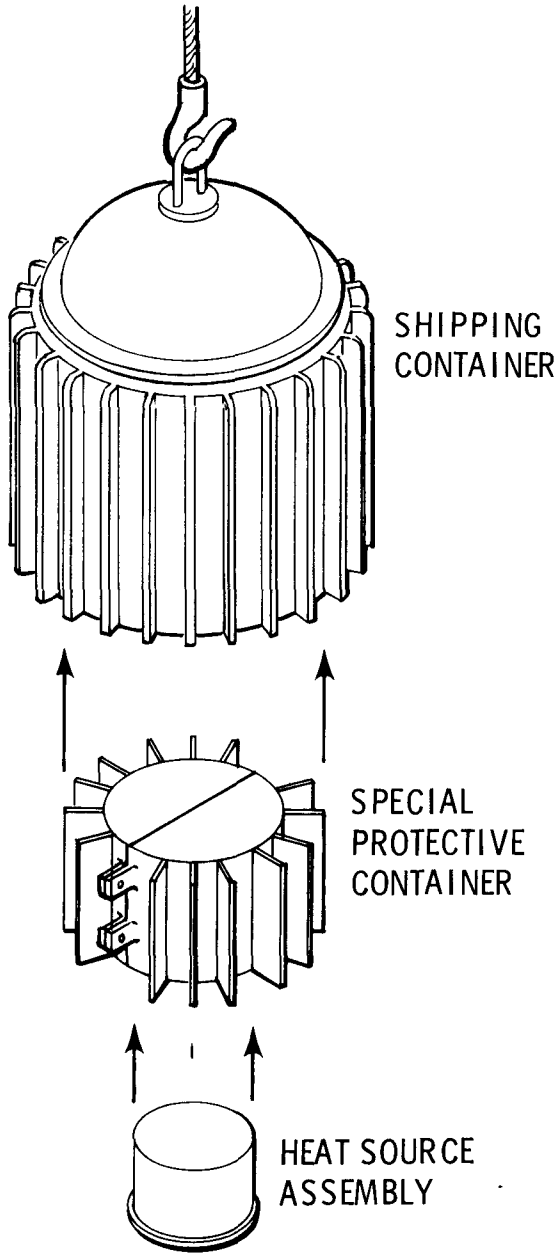

At the launch site the shipment is received by contractor personnel and transferred via a fork-lift vehicle or small crane (Figure 8) to a special nuclear material handling room in the payload operations building (4.0). There the HSA is removed from its shipping container and checked again for radiological integrity and thermal control operation. These operations are performed with the HSA inserted within an air- or water-cooled launch-site heat exchanger (LSHX). The LSHX can simply be a distribution duct which directs cooled air over the external surface of the HSA (5.0).

At this point testing of the refrigerator with the HSA installed can be performed within the payload operations building, if desired. Transfer of the payload to the launch pad should probably be performed with the HSA removed, however, due to the possible difficulty of cooling the latter within the payload structure, until the shuttle cooling system is accessible. The HSA would then be transported to the launch pad in a separate vehicle, still mounted to the portable LSHX (6.0).

At the launch pad, all payload elements are assembled in the payload change-out room prior to insertion into the cargo bay. This would provide the most convenient access to all sides of the payload and would be the preferred location for final installation of the HSA to the refrigerator, possibly through a local cut-out in the radiator (Figure 9). This would be the final step of the payload assembly process, prior to insertion of the payload into the cargo bay. Short periods without active cooling of the HSA are of no concern, because of its high heat capacity. The temperature rise without any cooling whatsoever is only in the range of 10-to-20^{o}F/min. Radiation and natural convection will tend to reduce this figure still further. Following payload insertion within the cargo bay, connection of the thermal shroud to the shuttle payload heat exchanger can be made.

Finally, the basic handling approach described can also be readily adapted to operations with disposable boosters. As before, the HSA is mounted as a final assembly step. In this case, the usual launchpad air cooler, suitably uprated in capacity, will keep the HSA exterior surface within proper tem-

Figure 8.
SHIPPING CONTAINER HANDLING TOOL

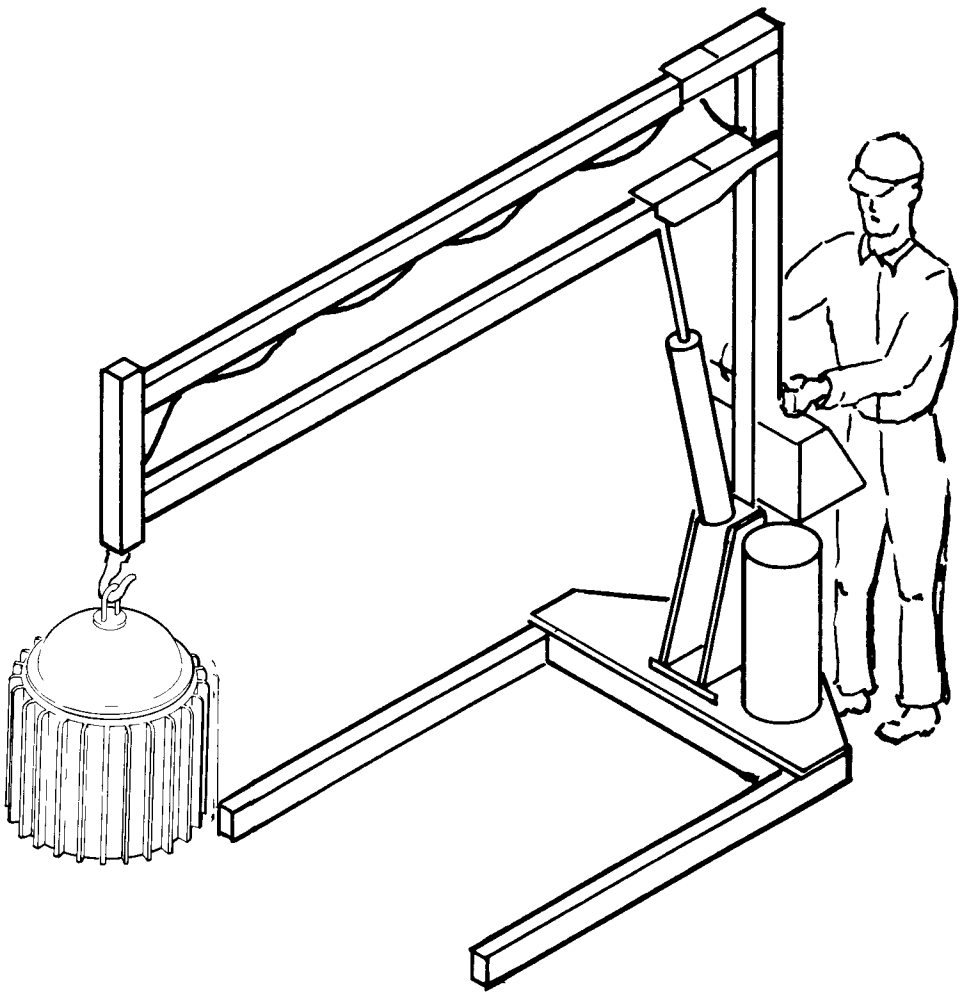

Figure 9.

ON-PAD LOADING OF HEAT SOURCE ASSEMBLY

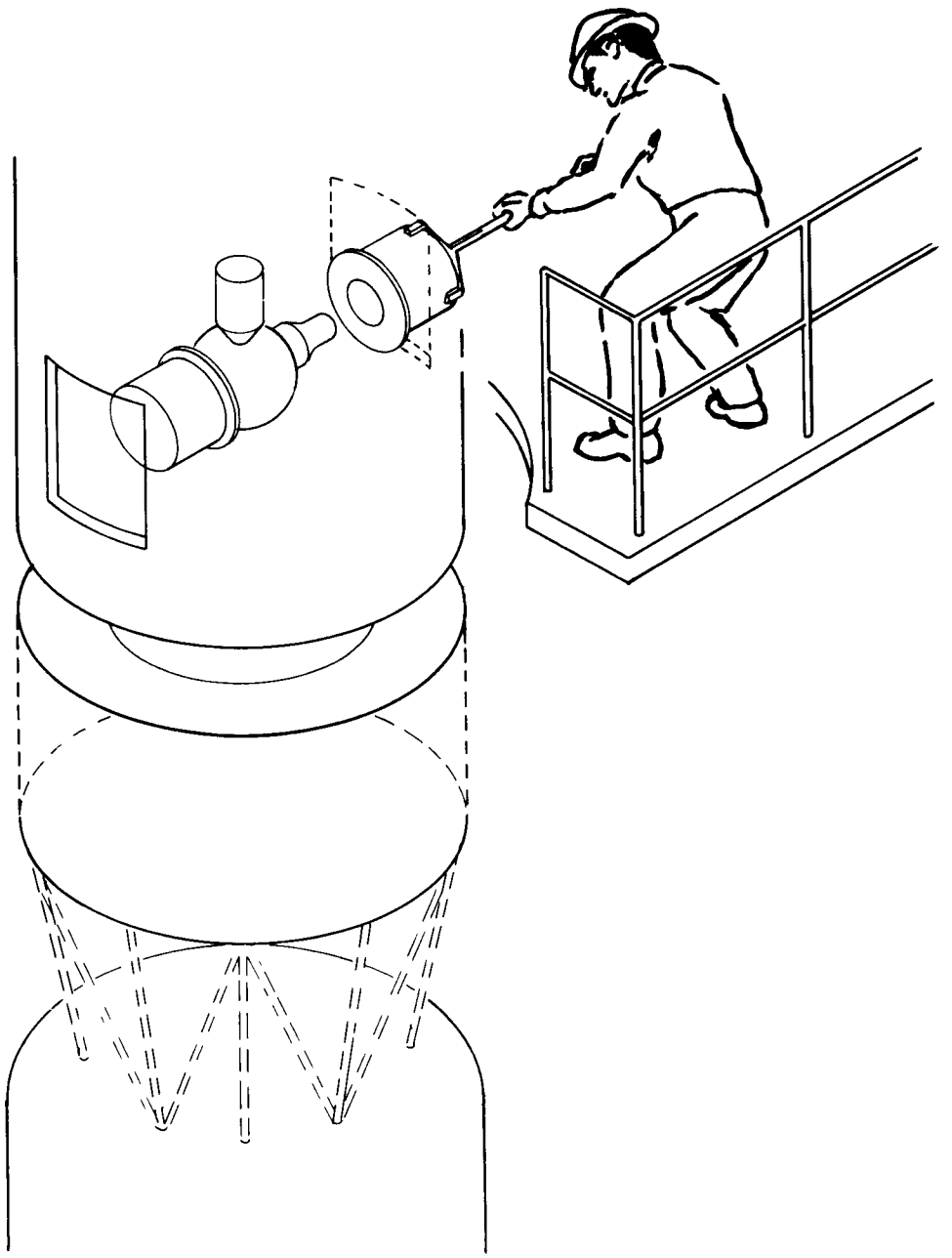

perature limits prior to the lift-off. After lift-off and umbilical disconnect of the air conditioning system, the temperature rise of the HSA will be negligible until the shroud is removed and the radiator is exposed. The refrigerator coolant pump can then be started, thus beginning active cooling of the HSA.

The command which starts operation of the refrigerator itself must be accompanied by a command which releases the solenoid valve on the heat source assembly, and vents the helium in the interfoil space, thus beginning space operations.

5.0 ADVANCED HEAT SOURCE DESIGN *

An advanced heat source design is described in this section which makes use of heat source technology currently in development for advanced isotope power programs. These programs are geared to the production of flight hardware within a 4-to-5 year development schedule. Heat source development activity will be generally concurrent with, although slightly in advance of, this schedule.

The heat source module described herein is an outgrowth of the Low-Cost High-Performance Generator (LCHPG) program. It employs the materials technology and safety considerations that are influencing new heat source developments for both advanced thermoelectric and dynamic power systems. The heat source module described below is based on the design approach currently favored for these power systems.

5.1 BASIC HEAT SOURCE MODULE

The building block for the VM engine heat source is the 225 watt module presented in Figure 10. As shown, this module contains 9 fuel capsules of 25 watts each. The radioisotope is pure plutonium oxide pressed into a cylindrical pellet, 0.898 in. diameter by 0.586 in. long. It is contained in a platinum-rhodium-tungsten alloy (Pt-3008) of 20 mils thickness. Each of the three groups of fuel capsules is surrounded by 0.100 inch pyrolytic graphite

* The work described in this section was performed by Teledyne Energy Systems, Timonium, Maryland under ERDA Contract SNSO-3

Figure 10.
CAPSULE HEAT SOURCE MODULE

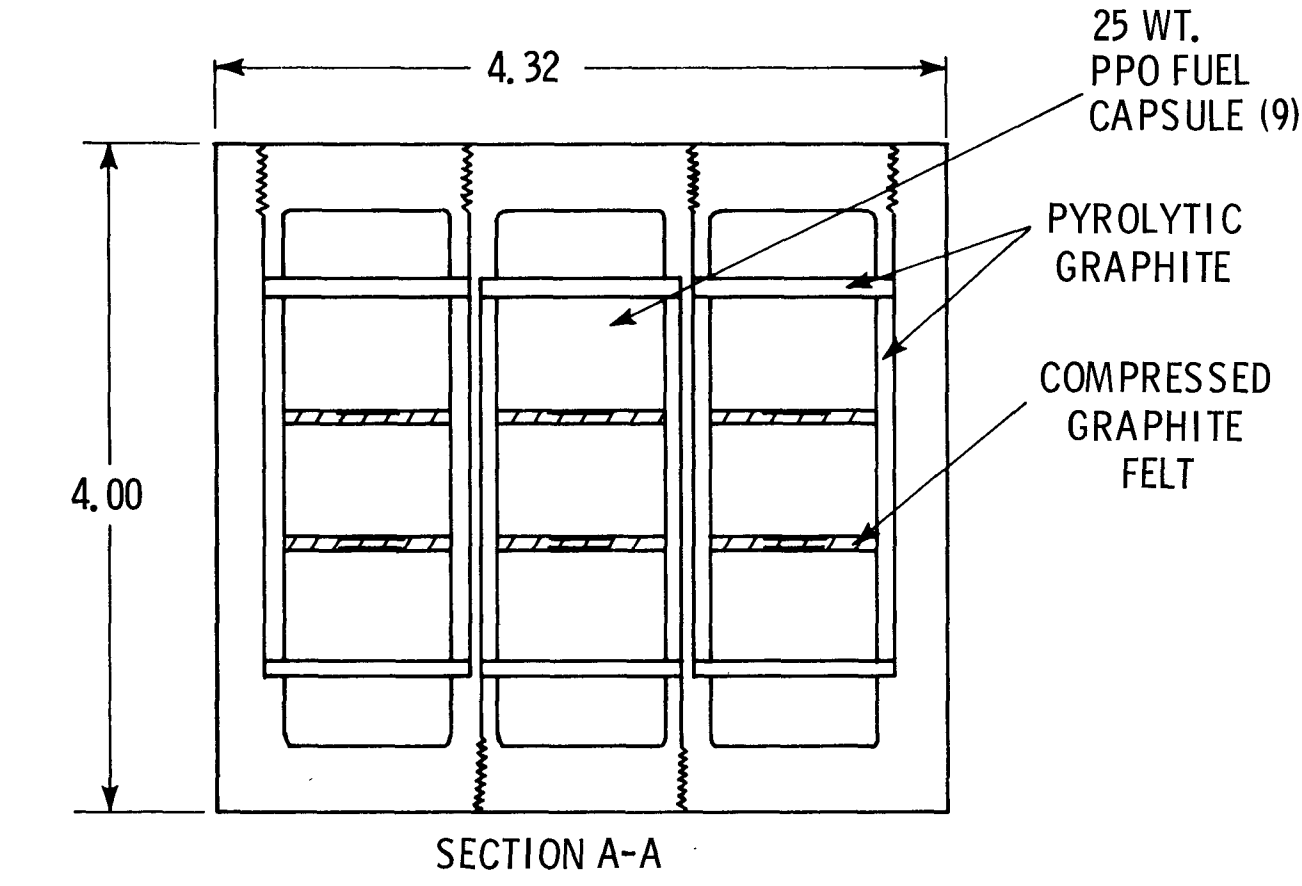

and the three capsules in a group are separated by compliant graphite felt. As indicated, the basic container and end plugs are made of graphite-graphite composite (3D graphite). However, the depicted threaded plugs are under investigation and an alternate closure may be devised if necessary.

5.2 CAPSULE HEAT SOURCE ASSEMBLY

The above heat source modules can be used with a multi-foil thermal control package, as described in section 2. To illustrate another possible thermal control alternative, Figure 11 shows a design using "fibrefrax" (quartz felt) insulation with variable-conductance heat pipes (VCHP) for thermal control. Such heatpipes contain a small amount of non-condensable inert gas, in addition to the condensable working fluid (i.e., sodium). Prior to sealing the pipe, the inert gas pressure is carefully matched to the working fluid vapor pressure at the desired switching temperature of the VCHP. Thereafter, at temperatures below the critical temperature the inert gas effectively prevents heatpipe operation by choking off vapor transport. At temperatures above the critical temperature the heat pipe operates by forcing the inert gas into a small reservoir at the condenser end of the pipe. Tests have shown that such heat pipes can automatically maintain a pre-determined temperature over a considerable range of heat source and heat sink variation.

The arrangement of five heat source modules around the VM engine cylinder shown in Figure 11 yields a nominal 1125 watts thermal input in a compact, easily installed configuration. In the design shown, fueling is accomplished by positioning the pentagonal array of heat source modules within a Pt-alloy container, on top of a ring of fibrefrax insulation. Subsequently, the covering assembly of insulation, heat pipes and emergency heat dump doors are lowered around the modules and bolted in place. This geometrical arrangement and assembly sequence allows pre-installation checkout of the thermal control systems.

During normal functioning of the refrigerator coolant loop the sodium-

Figure 11.
CAPSULE HEAT SOURCE ASSEMBLY

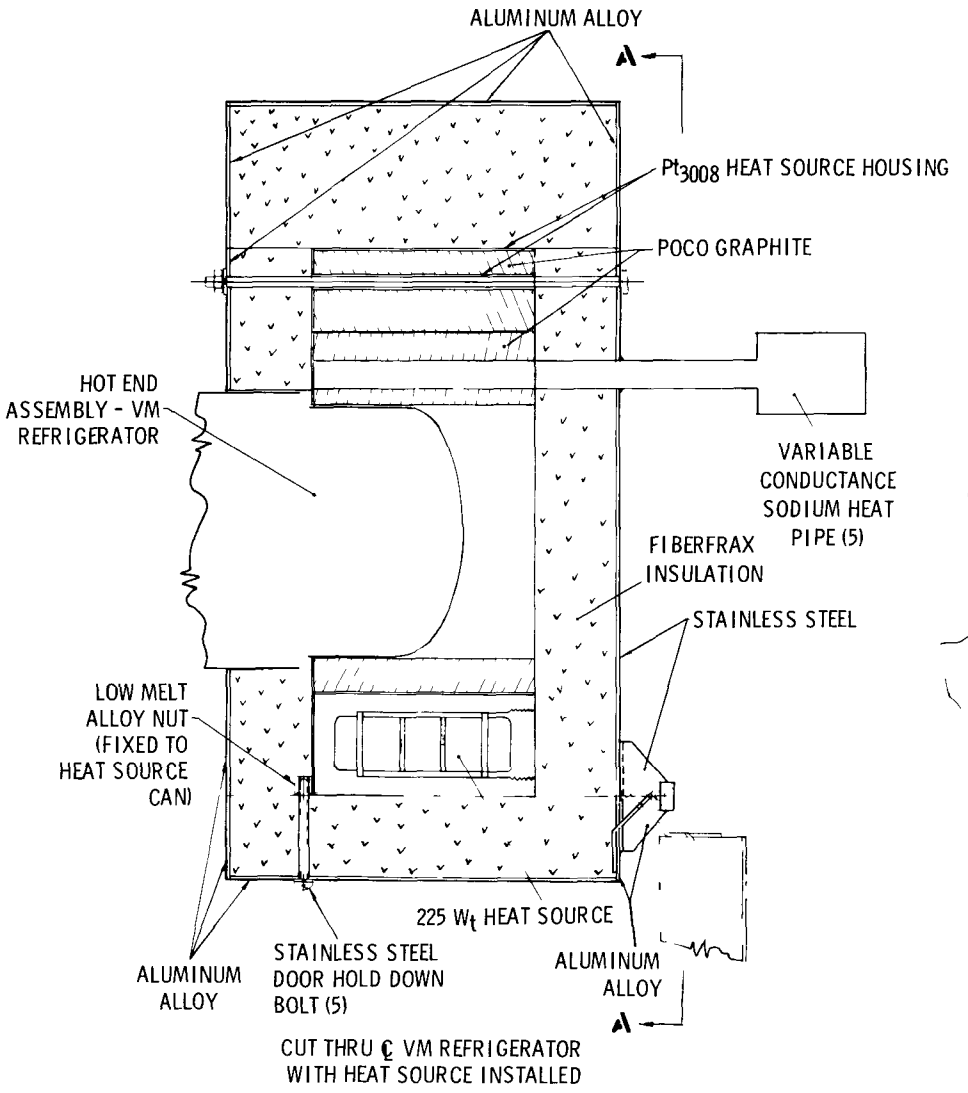

LEGEND

1 VARIABLE CONDUCTANCE SODIUM HEAT PIPE (5)
2 225 W_t HEAT SOURCE
3 POCO GRAPHITE
4 Pt_{3008} HEAT SOURCE HOUSING
5 FIBERFRAX INSULATION
6 STAINLESS STEEL
7 ALUMINUM ALLOY
8 LOW MELT ALLOY NUT (FIXED TO HEAT SOURCE CAN)
9 STAINLESS STEEL DOOR HOLD DOWN BOLT (5)
10 STAINLESS STEEL DOOR ACTUATING SPRING (5)
11 STAINLESS STEEL DOOR STOP (10)
12 STAINLESS STEEL HEAT SOURCE ASSEMBLY BOLT (5)
13 HOT END ASSEMBLY VM REFRIGERATOR

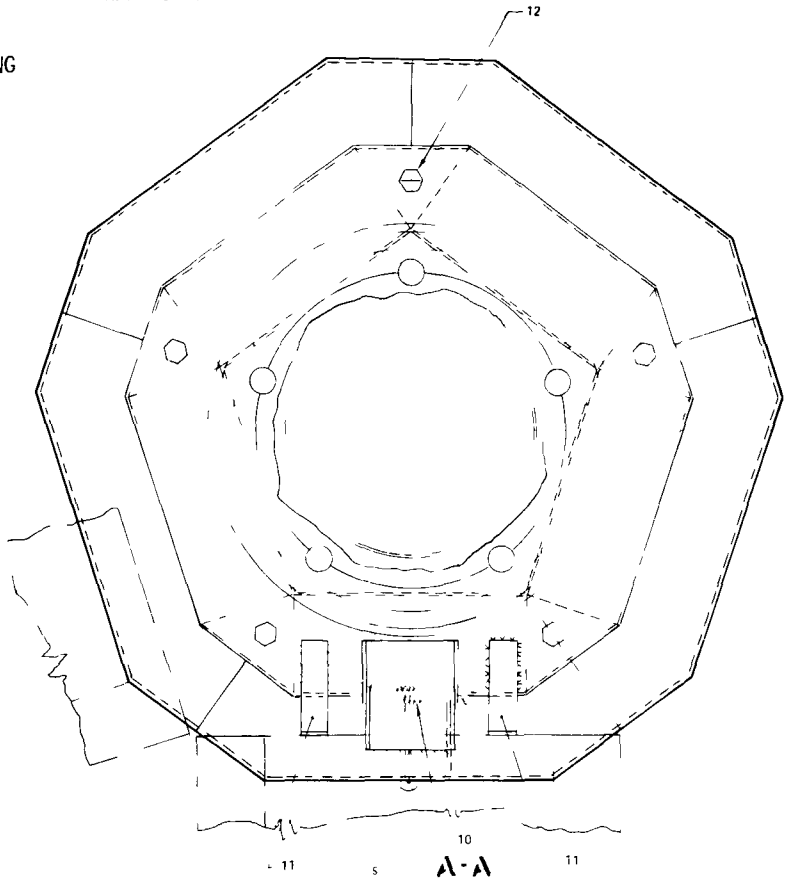

filled heat pipes limit the hot cylinder temperature to the specified operating temperature (1275°F), by radiating excess heat (if any) directly to space or to the surrounding thermal shroud. This control is effected regardless of the operating state of the refrigerator, as long as the heatpipes are functioning . In addition, there are emergency heat dump doors in the side insulation package which would be activated only if both the refrigerator and the heat pipes fail. In that event, as the heat source temperature rises to a pre-determined limit, a fusible link melts. This releases a tie-down strap, thus allowing the spring-loaded insulation doors to open. The opened doors allow direct radiation of heat to space or through an intermediate barrier/radiator suitably sized for acceptable overall thermal conductance to space.

The temperature of the hot cylinder wall and graphite, and the maximum fuel capsule temperature, are given in Table 3 for the normal VM engine operating mode (cylinder wall at 1275°F), as well as for the cases for the engine turned off and the heat pipes effecting thermal control, and for the emergency dump mode where no heat is assumed transferred to the engine or heat pipes.

Table 3 . Capsule HSA Operating Temperatures

	Normal Operation		Engine Off; Heat Pipe Control		Emergency Doors Open	
	°C	°F	°C	°F	°C	°F
VM Hot Cylinder Wall	690	1275	710	1310	510	950
Average Graphite	860	1580	880	1616	500	932
Fuel Maximum	900	1652	920	1688	550	1022

It is seen that during normal engine operation, the maximum capsule temperature is maintained at 900°C. When the engine is not operating, the variable conductance heat pipes maintain the cylinder wall and capsule temperatures (with small increase of 20°C) by dumping heat to space, or to the surrounding thermal shroud. The VM refrigerator can be readily re-started from this condition by re-starting the engine crank. In case of failure of both refrigerator and heat pipes, the emergency doors open and temperatures can be maintained well below their normal operating values.

The weights of all components shown in Figure 11 are listed in Table 4. It should be noted that the emergency doors only add about two pounds, since the side insulation is required to limit heat losses to less than 50 watts during normal operation. Also, the heat pipes contribute only about one pound, so that a doubling of the number of pipes for redundancy and/or temperature smoothing (if required) would add very little weight.

The major uncertainty attached to this thermal control approach is the long-term reliability and temperature-control stability of the VCHP's. Heat pipe operations within a rotating spacecraft might also present a problem if the axial g-forces exceed the wicking force of the pipe. If these problems can be overcome, however, the automatic operation of the system would simplify the command and control operations of the spacecraft.

Table 4. Alternative Design Weight Summary, 1125 w(t)

Component	Weight (lbs)
Heat Source Assembly (modules, enclosure, support)	22
Top and Bottom Insulation and Structure	3
Emergency Dump Doors (includes insulation and mechanism)	5
Heat Pipe Assembly (Heat pipes, graphite)	4
Total	34

References

1. SAMSO-TR-72-160, R.R. Murrel, A.J.Tomac, C.E. Sloan, et al, Final Report Spacetrack Augmentation Study I, Technical Analyses, Volume II, Philco Ford Aeronutronic, May 1972 (Secret)

2. C.E. Kelly, The MHW Thermoelectric Converter, Proceedings of the 10th IECEC, August 1975.

3. B.L. Renyer, High-Capacity, Long-life Vuilleumier-Cycle Refrigerator, Proceedings of the Cryogenic Cooler Conference, October 1973, AFFDL-TR-73-149.

4. Design Study of Rotary Thermal Compressor, R.W. Breckenridge, Jr., R.W. Moore, Jr., P.M. O'Farrell, A.D. Little Inc., AFFDL-TR-74-127. October 1974.

5. Development of a Heat Source Assembly for an Isotope Brayton Space Power Conversion System, Daniel Wein, General Electric, Co., 10th Intersociety Energy Conversion Engineering Conference (to be published).

6. Experimental Evaluation of an Automatic Temperature Controlled Heat Pipe, W.E. Harbaugh and G. Y. Eastman, Electronics Component Div. RCA. 3rd Intersociety Energy Conversion Engineering Conference, 1968. (Classified proceedings, since declassified).

APPENDIX A

Radioisotope Heat Sources -- A Summary of Characteristics

1. Design Evolutions

Radioisotopic heat sources have evolved in design over the years, driven mainly by the desire to minimize the environmental danger posed by a launch abort or premature re-entry from orbit. This is a continuing process, and it is expected that heat sources currently in production will be supplanted by more advanced designs now in the early stages of development. In addition to providing an increased safety margin against accidental occurrences, the newer heat sources are expected to be simpler and cheaper to manufacture. This should be particularly true for heat sources not required to operate above approximately 1000 C in temperature.

Under normal development conditions, the newer heat sources may be expected to be flight-ready within 4-to-5 years. "Normal" development implies continued mission requirements, but without an accelerated testing schedule which could probably be applied at increased funding levels, if necessary.

Although missions now scheduled for flight in the 1980's should be planned around the next-generation heat sources, a brief description of the present-generation heat source is provided, in part because the information is available in a more complete form at the present time, but also as a framework for discussion of the newer designs. Certain of the existing design features reveal requirements which will be carried over to the newer designs. Also, such items as radiation output, handling & shipping requirements, pad cooling requirements, etc., will be very similar to those currently in practice.

2. Present Generation -- MHW

The present-generation is represented by the MHW heat source (see figure). (The immediate past generation, SNAP-19, will have its last

launch under current plans, in the fall of 1975, as part of the Viking-75 mission. Coincidentally, the first MHW launch is scheduled to occur at approximately the same time, as part of the LES 8/9 mission.)

2.1 Design Description

The MHW heat source utilizes twenty-four spheres of plutonium dioxide to make up the 2400-watt (thermal) inventory. Each sphere is encapsulated in an iridium post-impact containment shell and is provided with its own impact protection. This assembly is referred to as a Fuel Sphere Assembly (FSA). The FSA's are arrayed in six planes along the length of the heat source, four FSA's to a plane, with each plane rotated 45 degrees with respect to the planes adjacent to it. The FSA array is contained within a POCO graphite aeroshell for reentry protection, which is also the basic structure of the heat source. The aeroshell is enclosed by an iridium outer clad which provides the mechanical and thermal interface of the heat source, pneumatic isolation of the heat source from its environment, protection during the multiple-skip class of reentries, and gas management for the helium generated by the fuel.

The heat source is designed to withstand all postulated accidents without fuel release. In addition, the nominal surface operating temperature is 1100 C. The combination of requirements of long-term fuel containment in the atmosphere (or undersea), and long-term materials compatibility in space at temperatures of 1100-to-1200 C, has led to the extensive use of metallic iridium as the fuel containment medium. Although, at the present rate of 650 dollars per thermal watt, the fuel itself is the major cost element, The high cost of high purity iridium, and the cost of forming it into matching hemispheres and welding it reliably, contribute to the relatively high cost of this heat source (see paragraph 2.3).

2.1.1 Fuel

The MHW heat source fuel is a stable ceramic compound, plutonium dioxide, which produces heat as a result of the alpha decay of plutonium-238. The total thermal inventory of 2400 watts is provided by 24 solid ceramic spheres of fuel, nominally 100 watts each. The function of the fuel is to pro-

MHW HEAT SOURCE

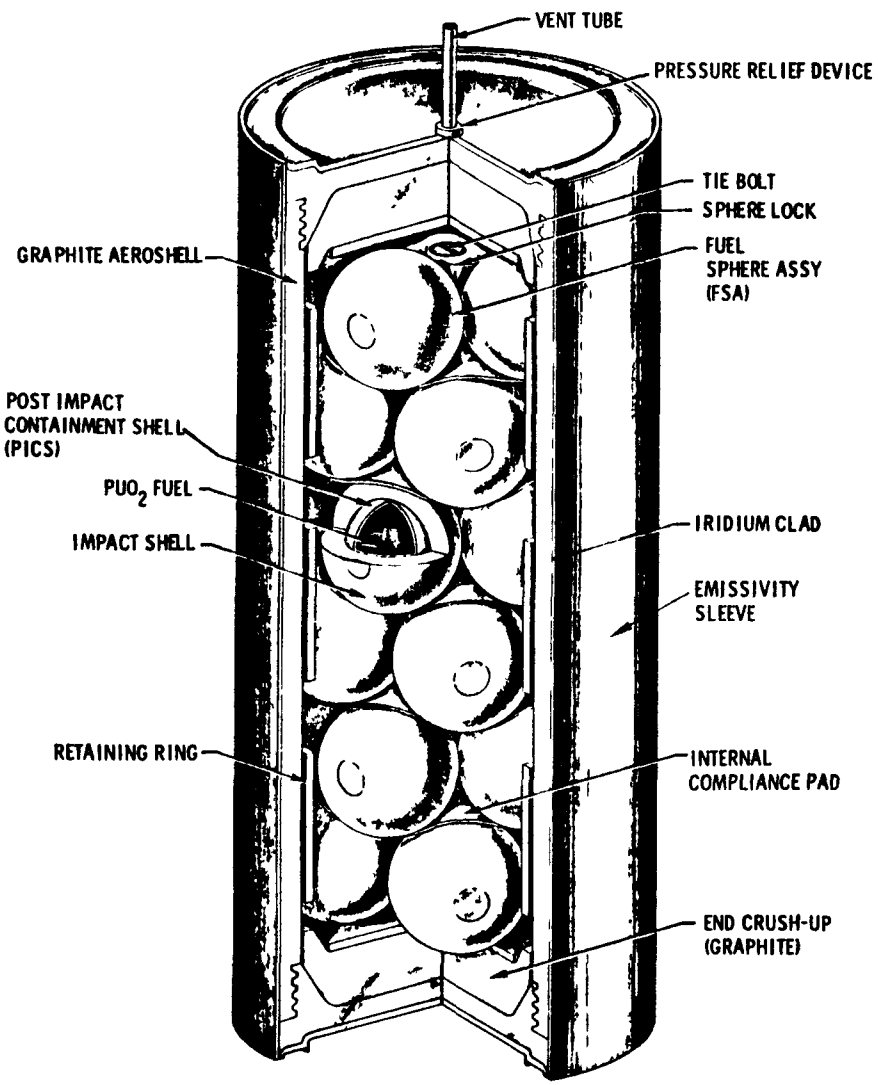

HEAT SOURCE (HS)

- THERMAL POWER 2400 ±30 WATTS
- LIFE
  - 1 YEAR STORAGE
  - 5 YEAR ORBIT OPERATION
- WEIGHT - 20.3 KG (44.68 LB)
- DIAMETER - 18.26 CM (7.19 IN)
- LENGTH - 43.10 CM (16.97 IN)
- VENTED TO SPACE

FUEL SPHERE ASSEMBLIES (FSA)

- $^{238}PuO_2$ CERAMIC COMPACT FUEL
- 24 FUEL SPHERES
- 100 WATTS$_t$ PER SPHERE
- 0.05 CM (0.02 IN) I_r SHELL (PICS)
- 1.17 CM (0.460 IN) T-50 GRAPHITE

AEROSHELL

- POCO GRAPHITE
- THICKNESS - 1.02 CM (0.4 IN)

IRIDIUM CLAD

- THICKNESS - 0.025 CM (0.010 IN)
- GRAPHITE OXIDATION BARRIER
- MULTIPLE SKIP RE-ENTRY CAPABILITY

EMISSIVITY SLEEVE

- T-50 GRAPHITE
- THICKNESS - 0.127 CM (0.05 IN)
- PROVIDES GOOD EMISSIVITY FOR NORMAL OPERATION

vide the heat energy which is utilized by the converter for direct conversion into electricity, the principal output of the MHW-RTG.

The alpha radiation produced by the fuel, because of its lack of penetration, does not constitute a hazard to human life unless the fuel is inhaled or ingested. The probability of inhalation or ingestion becomes non-zero as the result of an abort accident/reentry, and this is investigated in the MHW safety analysis task. However, the alpha particle reaction with light elements and spontaneous fission of plutonium combine to produce neutrons and gamma rays which can effect sensitive electronic equipment or human life if exposed at close proximities for long periods of time. Typical radiation dose rates are shown in paragraph 2.2 below.

As the alpha particles lose energy, they capture electrons and result in the production of helium molecules. This necessitates the incorporation of gas management considerations into the heat source design (see paragraph 2.1.6)

2.1.2 Post Impact Containment Shell (PICS)

The Post Impact Containment Shell (PICS), is a metal cladding which encapsulates each fuel sphere. It is designed to remain intact after exposure to all credible accidents, atmospheric reentries and impacts. The material of the PICS is a noble metal, iridium, which is one of the most non-reactive of materials. As a consequence, it is expected that the basically stable ceramic fuel will be contained for a long period of time within the iridium metal clad following any accident or reentry. The design requirement for the post-impact containment period is one year after impact.

In addition to its role as a "primary containment", the PICS provides a surface around the fuel which can be decontaminated after fuel encapsulation and which can be controlled dimensionally to a finer tolerance than the fuel sphere. Release of helium generated by the fuel is provided for by two vent holes in the PICS which are uncapped before final heat source assembly but after PICS decontamination. Retention of any fine particles of fuel which may exist within the PICS is accomplished by a particulate filter (a sintered iridium frit) within the PICS and underneath each vent hole. The total fuel plus PICS assembly is referred to as a Post-Impact Shell Assembly (PISA).

2.1.3 Graphite Impact Shell

The Graphite Impact Shell, (GIS), surrounds the PISA and is essentially a crushup structure which minimizes the deceleration loads during earth impact, so that the PISA can survive intact. Trade-off studies conducted earlier in the program determined that it was more advantageous to modularize the fuel and provide individual impact protection for each module rather than to provide one impact structure which protected the entire fuel inventory. This also had the effect of divorcing the design requirements for the impact shell from those of the aeroshell and allowed the choice of optimum materials and design for each component rather than a compromise. Consequently, the aeroshell's function ends at earth impact, at which point its size and shape determine the terminal velocity of the total heat source assembly. Thus, the impact shell is designed to protect the PISA during the impact at the heat source's terminal velocity (plus a 10 percent margin for uncertainties). The assembly of the PISA and its impact shell is referred to as a Fuel Sphere Assembly (FSA).

2.1.4 Aeroshell

The aeroshell is an assembly consisting of an ablator cylinder with end caps. The aeroshell is the basic structural member of the heat source assembly and contains all of the other heat source components with the sole exception of the outer clad/gas management assembly. The ablator is designed to maintain the structural integrity of the heat source from assembly through all credible events (with the exception of some booster explosion situations) to the moment of earth impact following a reentry or an abort. The ablator also provides the heat source aerodynamic shape and thus defines its reentry behavior (heating, ablation, terminal velocity, etc.).

2.1.5 Outer Clad

The outer clad is a metal envelope which surrounds the heat source aeroshell. The four primary functions of the outer clad are:

1. Provides pneumatic insulation between heat source and converter
2. Provides oxidation protection to the graphite aeroshell
3. Provides skip reentry capability
4. Provides the capability of maintaining a helium environment within the IHS for heat transfer purposes.

The first function of pneumatic isolation precludes any interactions which could arise due to gaseous species produced by either device.

The second function protects the graphite aeroshell and other IHS internal components from oxidation and any other deleterious effects from ground handling of the IHS in air environment prior to installation into the converter.

The third function protects the ablator from the large surface recessions inherent in the multiple skip class of reentries (those having either too high a velocity or too shallow an entry angle to be captured on the first entry). The ability of this outer clad to remain intact from 3500^{o} to 4000^{o} F eliminates the need for a 0.2 to 0.5 inch of extra ablator thickness.

The fourth function, coincident with the gas management system, provides a capability to utilize the helium generated by the fuel to reduce internal temperatures within the heat source.

The clad also provides the mechanical interface to the heat source.

The outer clad material which satisfies these functions is a noble metal, iridium.

The outer clad is encased in an "emissivity sleeve", a tight-fitting graphite sleeve which provides some structural support for the thin metal and enhances the radiative heat transfer to the thermopile hot junctions. The outer clad end caps furnish the bearing surfaces for support of the IHS within the converter.

2.1.6 Gas Management System

The gas management system (GMS) vents the fuel-generated helium from the heat source outboard of the converter. The GMS is comprised of tubulation from the IHS outer clad through the converter outer case, a ground handling vent valve, and either a Pressure Relief Device (PRD) or a Pressure Maintenance Device (PMD). The PRD is a barometrically-operated device which relieves essentially all helium pressure within the IHS during space operation. The PMD maintains slight helium pressure (1 or 2 psi) within the IHS throughout operation to minimize internal temperatures.

2.2 Nuclear Radiation Output

For PuO_2 fuel, neutrons are produced mainly from α, n reactions with oxygen. Neutrons are also produced from spontaneous fission at an order-of-magnitude lower rate. Maximum neutron energy from the α, n reaction is 5.8 MeV, with a spectrum extending down to very low energies.

Gamma rays are produced mainly from spontaneous fission. Table 1 below shows the measured radiation from a fully-fueled (2400 W_t) MHW generator. The distance is measured from the center of the isotope heat source (IHS)* (See Appendix B page B 12 for data on a flight heat source.)

Table 1 - Q-1 RTG Radiation Survey

Distance (IHS center in meters)		Dose Rate - mrem/hr		
		GAMMA	NEUTRON	TOTAL
side	0.20	130	780	910
	1.	7	42	49
	1.5	3	22	25
	2	2	13	15
top	0.34	36	216	252
	0.44	19	120	139

* Bi-Monthly Progress Report, MHW-RTG Program, Period 1 March to 30 April, 1974

Generally, the maximum permissible occupational dose rate permitted in adults is 3 rem per calendar quarter. Therefore a distance of one meter or more, normal work activity can proceed for several hours per week, although portable shielding is an obvious preference. Generally, RTG mounting is accomplished by a hoist or fixture which permits operator removal of several feet. Tie-down or bolt-tightening can be accomplished by technicians in several minutes without exceeding the occupational dose limits.

2.3 Cost

With the cost of fuel reckoned at 650 dollars per thermal watt, the recurring cost of the MHW heat source is estimated at 1000 dollars per watt(t). It has been estimated that future production costs of Pu-238 could be reduced to 300-to350 dollars per watt(t) by about 1980, providing: 1.) Np-237 feed material is available from commercial sources at $30 per gram, and 2.) user requirements for Pu-238 increase to 60-120 kg per year (33-66 kWt/yr).* (Current production is ~ 30 kg/yr).

Such a reduction in fuel cost will reduce the MHW HS cost to approximately $700/$W_t$.

3. Future Heat Sources

3.1 Objectives & Approaches

Two major improvements are expected to be achieved in the heat source development program now underway:

1. Cost reduction
2. Safety margin improvement

The first objective is expected to be achieved by using a platinum-rhodium alloy (Pt-3008) as the oxidation-resistant fuel containment medium. This material is lower cost, more readily available, and easier to work than high-purity iridium. Its maximum operating temperature may be limited

---

* letter dated 6 June 1974, Dixy Lee Ray (Chrpsn, USAEC) to Hon. Malcolm R. Currie (Dir. DDR&E)

to 800-to-1000 C depending on tests now underway; however, this will not be a severe limitation for many applications.

Also, cost reduction will be further enabled by avoiding the intricate fabrication of spherical shapes and by standardizing on a uniform cylindrical fuel capsule for all applications. The latest design version of this capsule containing a nominal 25 watts(t) of fuel, is shown in the attached figure.

These capsules will be inserted into graphite aeroshell blocks (POCO or 3D-graphite), to produce the heat source module. The heat source is then built up by stacking modules. However, in contrast to the MHW HS, each module is designed to re-enter separately. This results in a low ballistic coefficient for the modules, and hence a much reduced impact velocity, thereby achieving the second of the major improvement objectives.

Low ballistic coefficient aeroshell modules can be achieved in a number of design variations, depending on the application. The attached figures show a number of possibilities, each designed for a different requirement. Obviously, other variations are possible, within the constraints of the ballistic coefficient and heat transfer requirements.

The completion of a heat source from these modules will require a means for stacking and supporting the modules within an enclosing structure, possibly a superalloy, depending on operating temperature requirements, and a gas management system similar to that of the MHW HS.

3.2 Nuclear Radiation

Nuclear radiation output from a heat source of the same thermal power would be only a slightly greater than that measured for the MHW-RTG (Table 1) since the converter itself interposes only minimum shielding, particularly for neutrons.

3.3 Cost

The costs of these advanced heat sources can be only guestimated

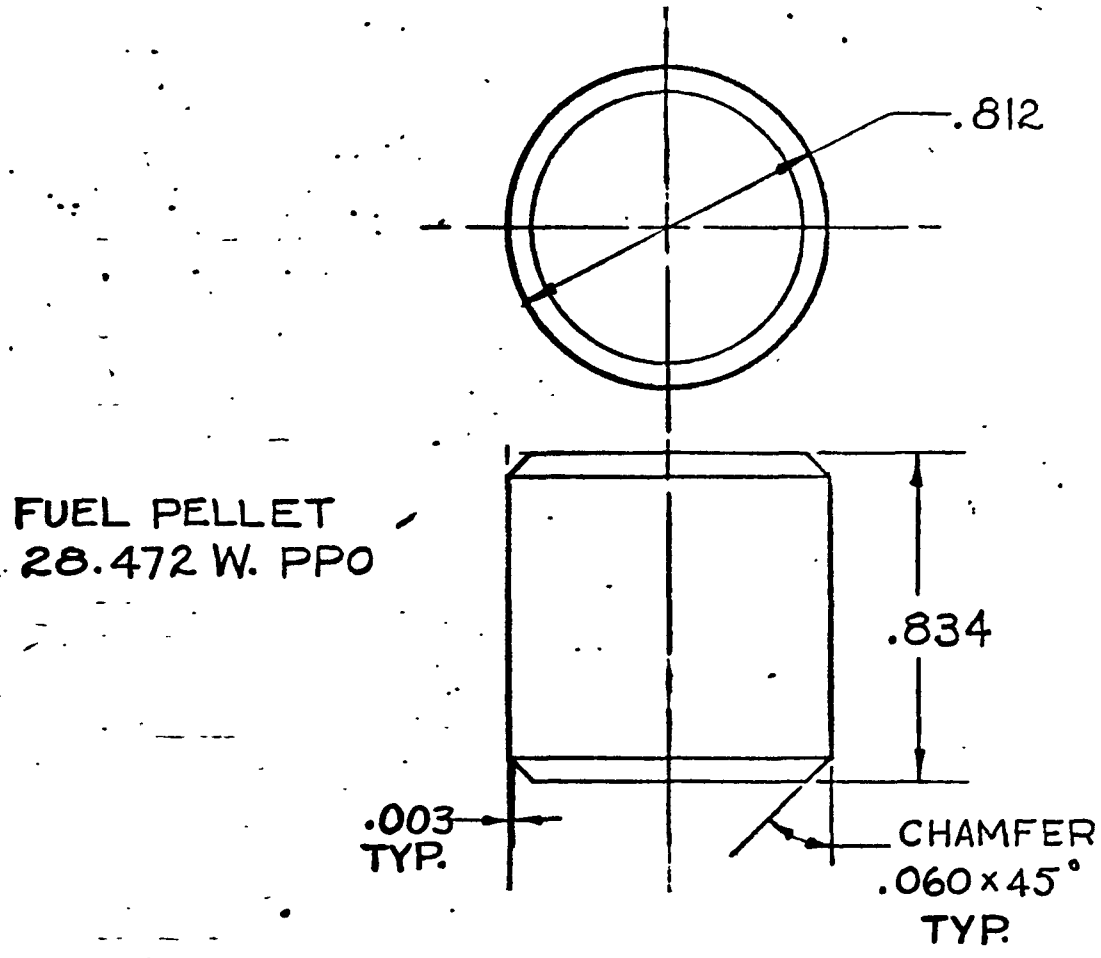
.812
FUEL PELLET
28.472 W. PPO
.834
.003
TYP.
CHAMFER
.060 x 45°
TYP.

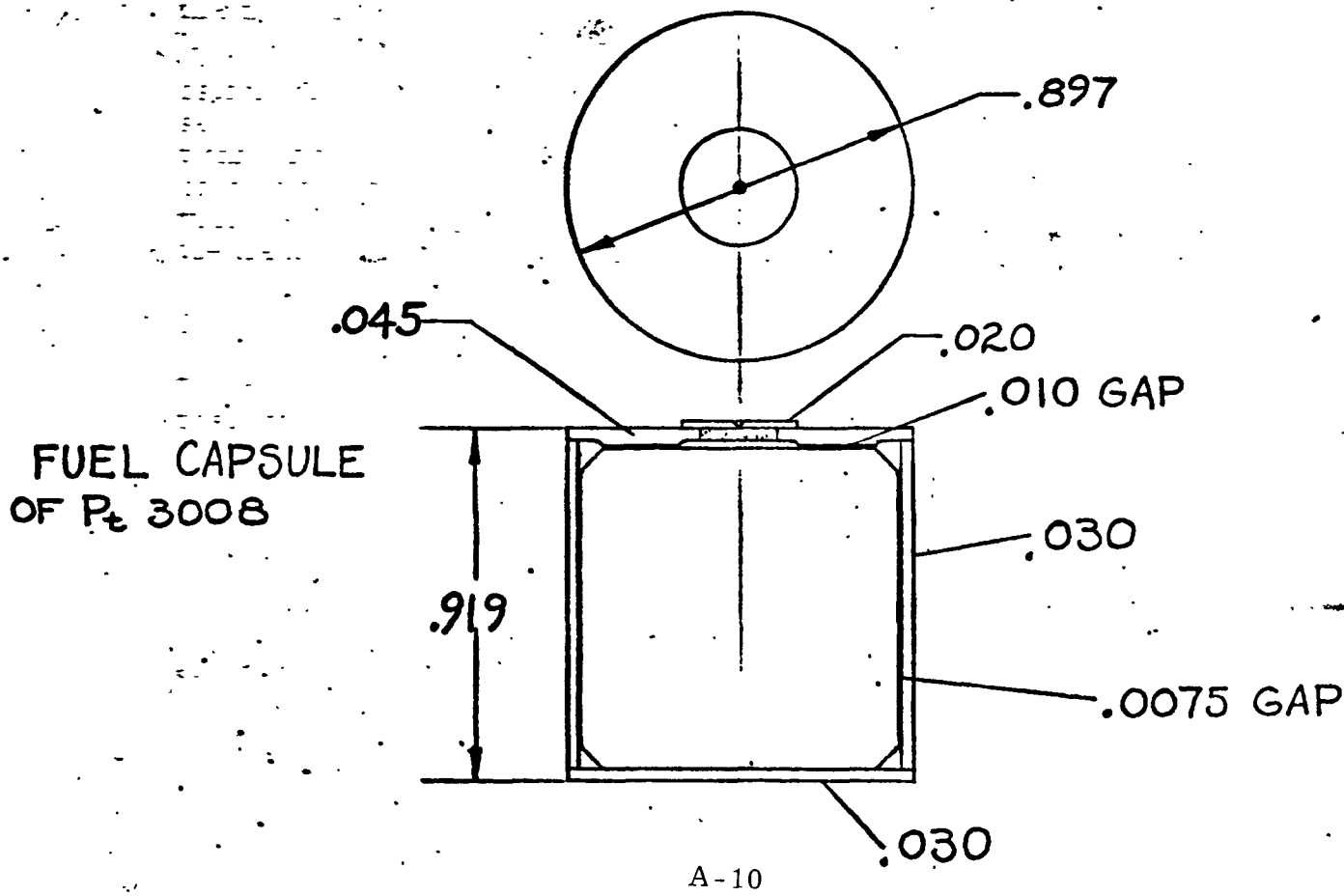
.897
.045
.020
.010 GAP
FUEL CAPSULE
OF Pt 3008
.030
.919
.0075 GAP
.030

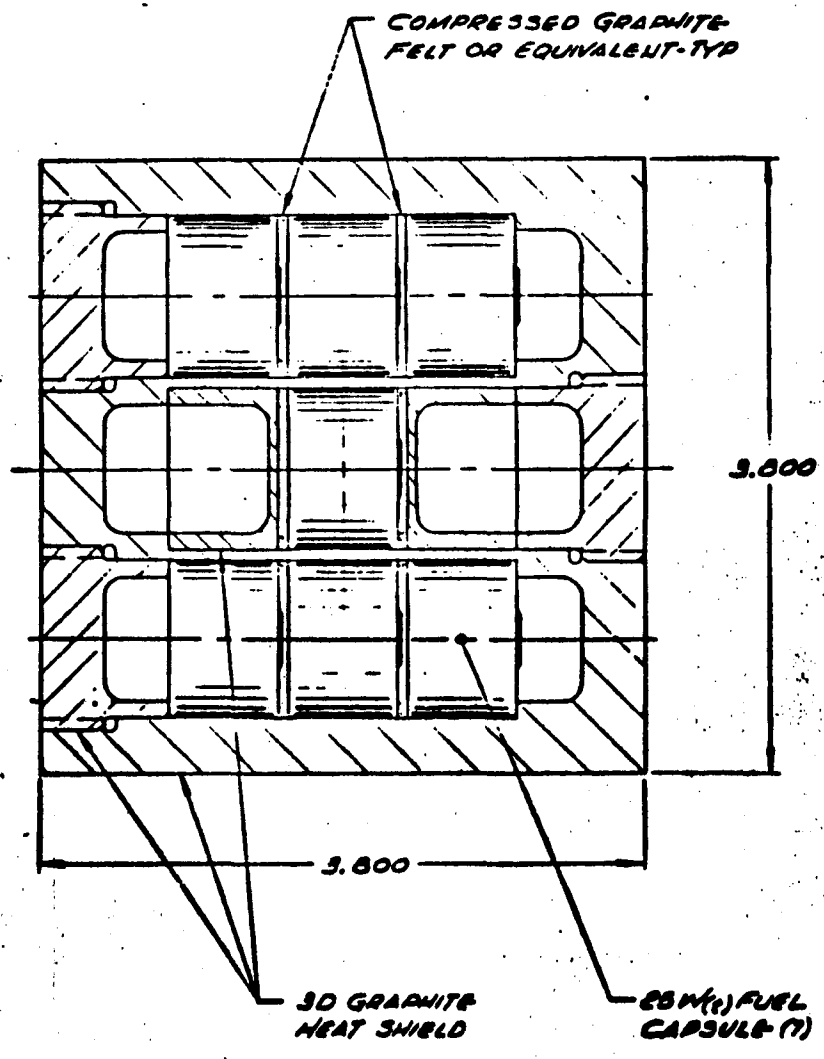

SECTION A-A

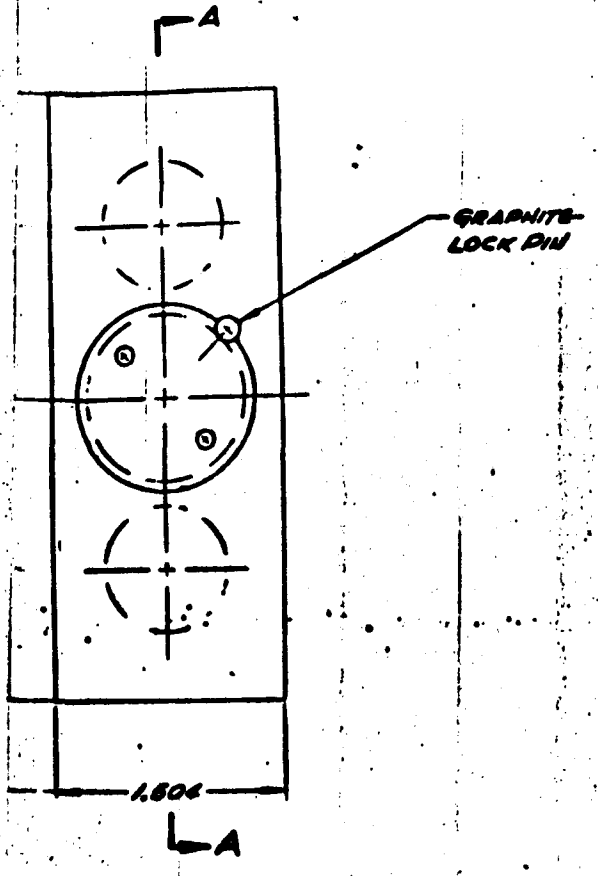

MODULE WEIGHT = 2.38 LB

THERMAL POWER = 175 W_t

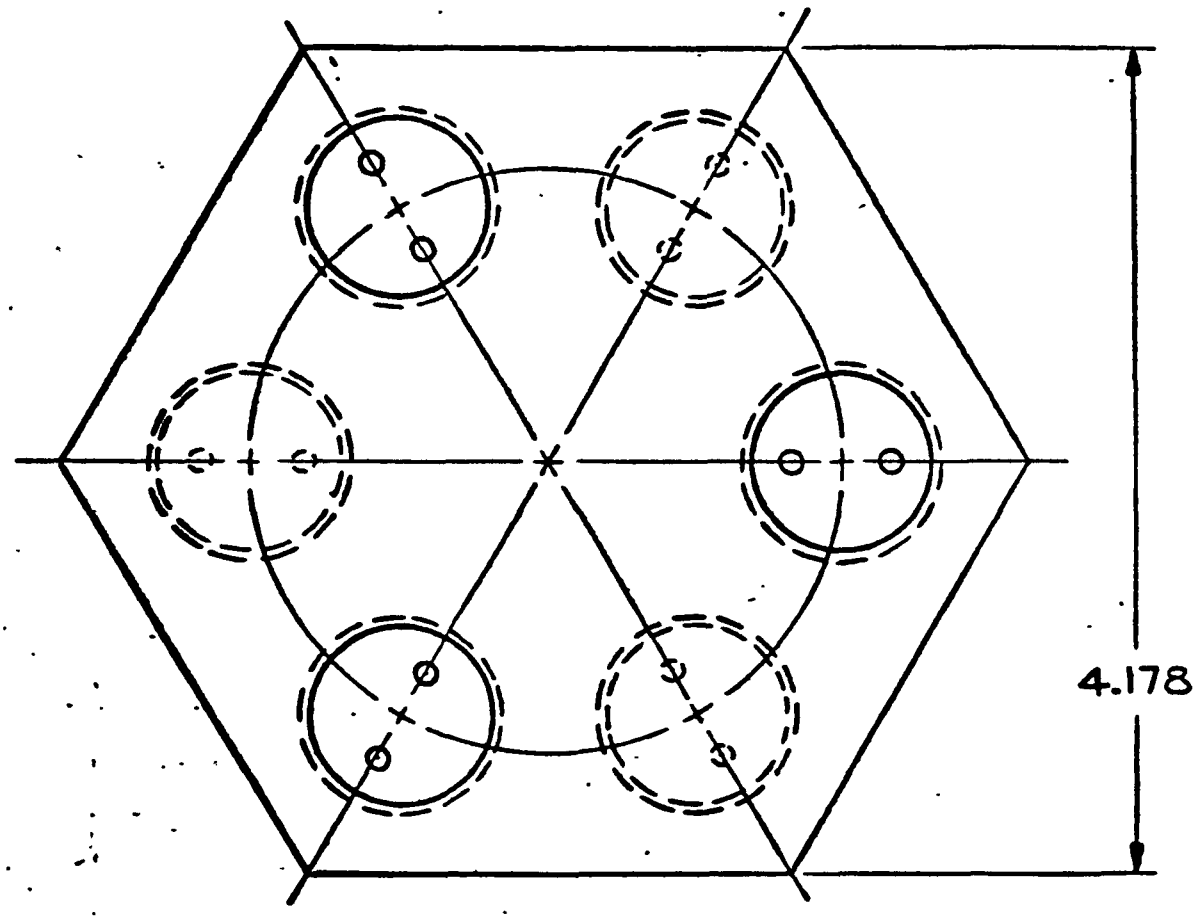

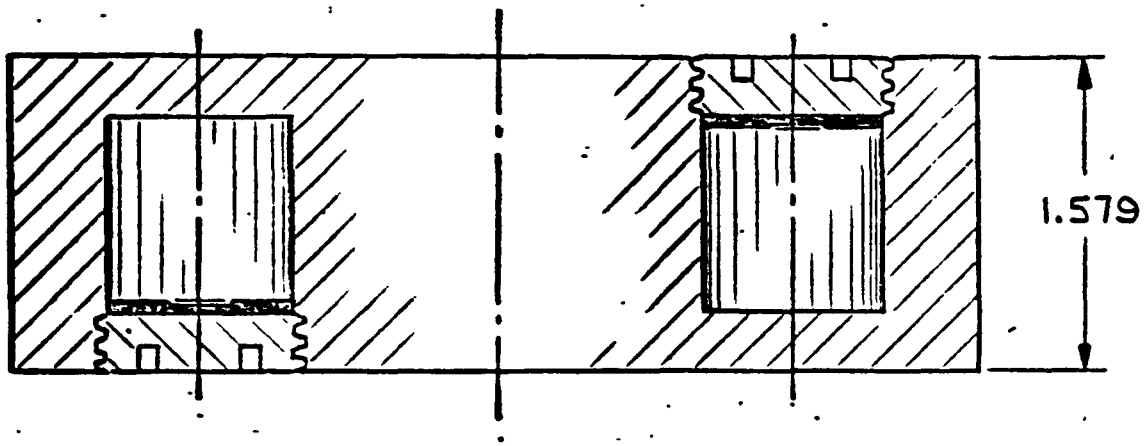

HPG S/N 1

HEAT SOURCE MODULE

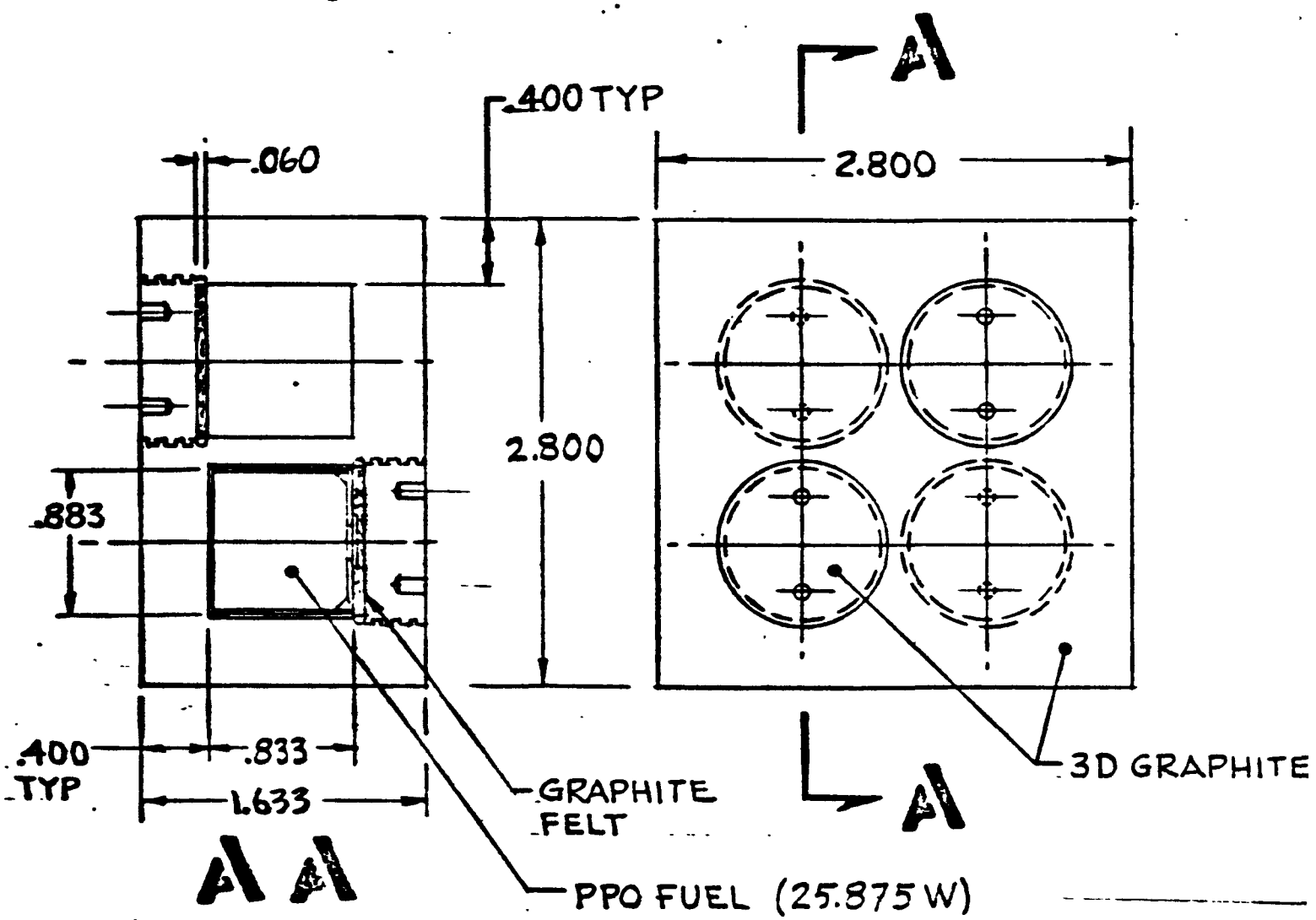

HEAT SOURCE UNIT

at the present time. Assuming a fuel cost of $350 per watt(t) (1973 dollars), total heat source costs should be in the range of $500-to-750 per watt(t).

APPENDIX B

Plutonium-238 Radiation Data

The following is a compendium of information on pure plutonium oxide (PPO) fuel and its radiation characteristics.

Some of the attached data sheets have been simply reproduced from original source documents; the sources are identified by reference numbers in square brackets.

1. Fuel Data

Pages 2 and 3, reproduced from reference [1], contain useful summary information on the most current fuel form, now manufactured for the MHW-RTG. This should be used as background information only; note that the gamma ray data does not include the important decay-product radiation which is time-variable.

Also note the statement regarding neutron radiation in paragraph 3.g. The current standard fuel is manufactured from oxygen enriched in ^{16}O to reduce the neutron contribution due to α,n reactions in the ^{18}O isotope Current specifications call for a minimum of 99.98 percent oxygen-16 in the feed gas. (Natural abundance is 99.76% ^{16}O.)

1. Plutonium Content of Typical $^{238}PuO_2$ (80 at%) produced at the USAEC Savannah River Plant

a. Plutonium Isotope

	wt%	Half Life (yr)
^{236}Pu	~0.001	2.8
^{238}Pu	80(1)	87.80 ± 0.02
^{239}Pu	16.5	2.4×10^4
^{240}Pu	2.5	6.6×10^3
^{241}Pu	0.8	13.0
^{242}Pu	0.1	3.7×10^5

b. Pure Plutonium Oxide (PuO_2)

Pu	88.15
O	11.85

c. Impurities

The analyses reported in the following section represent averages of analytical studies carried out by LASL on typical MRC Flight Quality specimens.

1) Actinide Impurities

Element	wt%
Th	0.29
U	0.64*
Np	0.12
Am	0.05

2) Common Impurities, Specified and Determined

Element	Specified Impurity Level, (ppm)(2)	Typical Analyses (ppm avg.)
Al	150	50
Ca	300	200
Co	50	30
Cr	250	85
Cu	100	5
Fe	800	300
Mg	50	20
Na	250	40
Ni	150	15
Pb	100	5
Si	200	160
Sn	50	15
Ta	200	100
Zn	50	10
C	---	250

*^{234}U grows in at the rate of ~525 ppm/mo as a result of the decay of ^{236}Pu. Therefore, the U content is a function of the age and initial isotopic composition of the particular specimen.

2. Calculated Power Factors (Based on 0.453 w/g of total Pu)

a. 0.399 watts per gm

b. 12.1 curies per gm

c. 30.4 curies per watt

d. Note: The above values are calculated based on pure 100% dense $^{238}PuO_2$ with 80 at% enrichment in the 238 isotope. From the specified diameter and thermal inventory of a typical sphere, one may then calculate an "effective" sphere power density as 3.71 ± 0.2 watts/cc.

3. Radiation

In describing radiation from 80 at% $^{238}PuO_2$, several factors must be considered: (1) whether the values are based on an unshielded or shielded source. For example, a significant L X-ray emission rate is associated with ^{238}Pu. However, the energy is low (0.015 MeV) and these X-rays are easily absorbed by ordinary thicknesses (~0.030 in.) of common encapsulating materials such as stainless steel or Ta, (2) actual percentages of both other Pu isotopes and actinides. For instance, the ^{236}Pu content is specified(1) as ≤ 2 ppm; typical Savannah River oxide averages 0.6 - 1.2 ppm. However, the exact value is a function of the processing history of the particular "batch" and may vary from lot to lot. The isotope ^{236}Pu has ^{208}Tl in its decay chain; ^{208}Tl has an energetic gamma (2.6 MeV) which grows in as the ^{236}Pu decays. The varying amounts of Th, U, Np, and Am also contribute to the gamma spectrum. Therefore, a variety of qualifications must be considered in a tabulation of radiation characteristics. To avoid these ambiguities, unless otherwise specifically stated, the data in sections 3.a through 3.c refer to ^{238}Pu only.

a. Alpha

	Energy (MeV)	Particles/watt-sec
1.	5.491	7.95×10^{11}
2.	5.448	3.20×10^{11}
3.	5.352	1.5×10^9
4.	5.200	5.0×10^7
5.	5.000	7.0×10^4
6.	4.700	1.3×10^6

b. Beta - None

3. (cont'd)

c.

Gamma	(keV) Energy	Gamma-Ray Intensity (gammas per alpha)	Avg. Std. Dev. (%)
1.	15.0	0.13	-
2.	43.5	2.51×10^{-4}	1
3.	99.6	7.66×10^{-5}	1
4.	152.5	8.5×10^{-6}	1
5.	201.2	4.3×10^{-8}	2
6.	707.8	3.3×10^{-9}	7
7.	742.4	5.25×10^{-8}	1
8.	765.8	2.31×10^{-7}	1
9.	785.8	3.3×10^{-8}	2
10.	807.6	8.5×10^{-9}	5
11.	851.3	1.36×10^{-8}	1
12.	882.9	9.4×10^{-9}	2
13.	926.5	5.3×10^{-9}	1
14.	941.8	5.3×10^{-9}	4
15.	1001.1	9.5×10^{-9}	1
16.	1041.8	2.2×10^{-9}	8
17.	1085.1	7.0×10^{-10}	9

d. Bremsstrahlung - Negligible

e.

Neutrons[3]	Source	(MeV) Energy	Emission Rate, n/sec/g Pu(Total)
1.	Spontaneous Fission	0 - 10 (Avg. = 2.0)	2200
2.	α/n Reactions, light elements only. At Z = 14, the coulomb barrier reaches 5.5 MeV		See Table I

f. Specified Emission Rate[2] for Typical Sphere: 8×10^3 n/sec/g Pu (Total). This includes self-multiplication factor of 1.18

g. Typical Determined Emission Rate on MRC Flight Quality Spheres: $5.0 \pm 1.0 \times 10^3$ n/sec/g Pu (Total)

TABLE I[3]

Specific Neutron Yields from Light Element Impurities in ^{238}Pu

Element	n/sec/g ^{238}Pu for 1 ppm
Li	5.7
Be	162
B	51
C	0.2
O	0.1 (natural mixture)
^{17}O	0.62
^{18}O	6.25
F	22
Na	2.7
Mg	2.6
Al	1.2
Si	0.2
P	< 0.03
S	< 0.03

Note that "normal" oxygen in $^{238}PuO_2{}^{nat}$ could contribute significantly to the overall emission rate. However, the mass-16 oxygen isotope does not undergo the α, n reaction to any practical extent. Therefore, if $^{238}PuO_2{}^{nat}$ is enriched in ^{16}O, the contribution to the overall neutron emission rate may approach that of the spontaneous fission rate of the nucleus. The "efficiency" of this enrichment, or exchange, depends upon a variety of processing parameters. Typical $^{238}PuO_2{}^{nat}$ has an emission rate of 12,500 n/sec/g Pu (Total); the spontaneous fission rate is 2200 n/sec/g Pu (Total. Section 3.g above indicates a nominal emission rate of ~5000 n/sec/g Pu (Total) for a Flight Quality Sphere.

h. Dose Rate

A more meaningful value associated with radiation is a typical dose rate (β, γ) from a Flight Quality MHW Sphere. This value now includes the contribution from various plutonium isotopes, other actinides and all daughters. Dose rates are usually measured at 10 cm from the encapsulated source. Using MRC MHFT-17, a dose rate of 0.2 mr/hr was measured at 10 cm through 0.020 in. of Ir.

2. Neutron Data

2.1 Source Term

The relative spectral distributions of the three major neutron sources can be seen in figure 1. [2] Note however, that this figure is for un-enriched oxygen and for fuel which does not meet the purity standards shown in page 2. The values of the (α, n) reaction curves are reduced by approximately an order of magnitude with current standard fuel.

2.2 External Radiation

Table II shows the calculated neutron spectral distribution at a detector point located 1 meter from a current standard 2400 watt(t) MHW-RTG. The detector is located at a point normal to the generator axis (90^{o}).

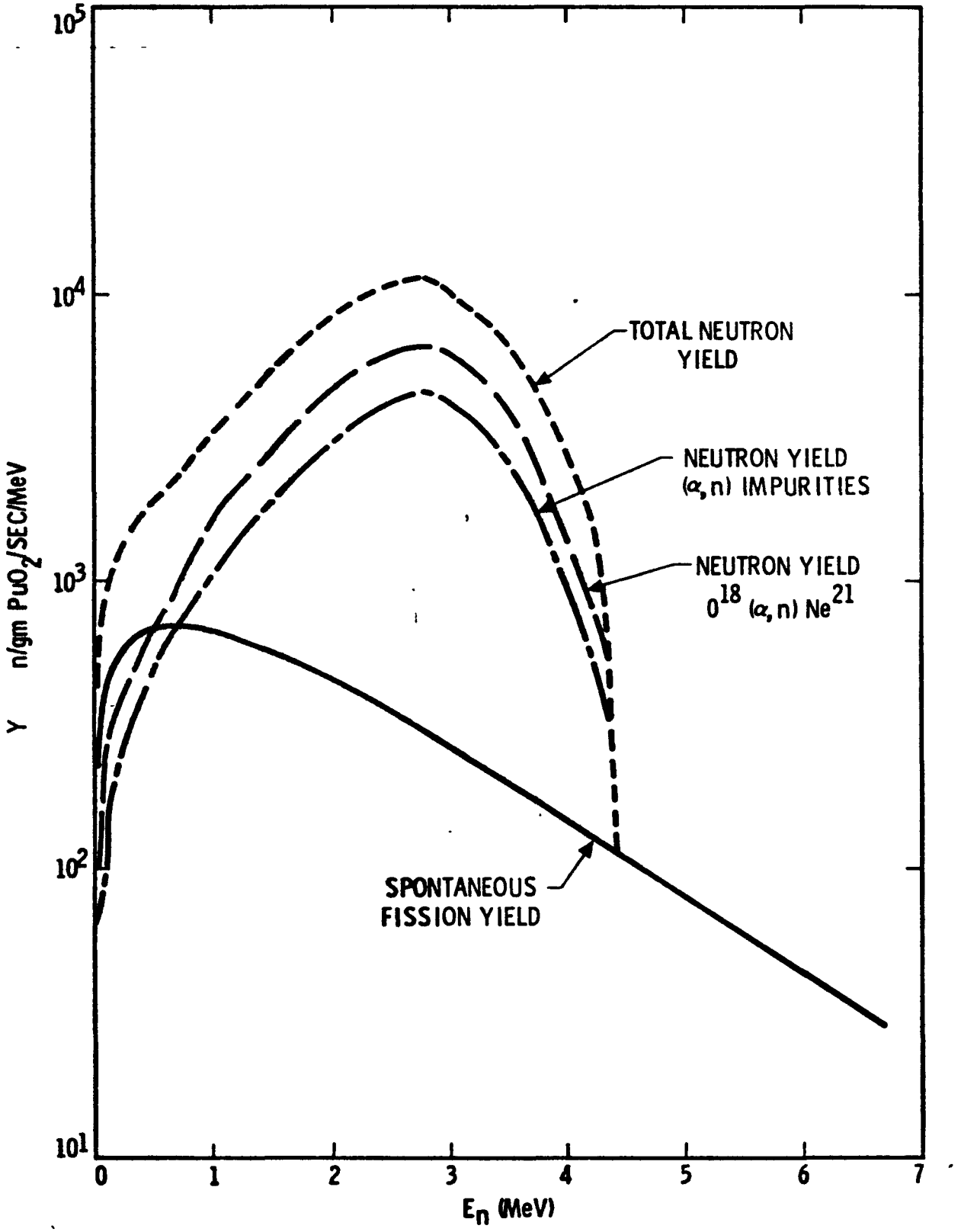

Figure 1. Total Neutron Yield from a 2.2 kW MHW PuO_2 Source [2]
(Not enriched or purified to current standards)

Table II [3]

MHW-RTG Neutron Spectrum @ 90^{o}, 1 meter from center of RTG

Energy (MeV)	n/cm^2 - sec - MeV	n/cm^2 -sec
10.0 - 8.55	0.437	0.63
8.55 - 6.66	1.49	2.8
6.66 - 5.18	3.9	5.8
5.18 - 4.46	8.35	6.0
4.46 - 4.04	17.	7.1
4.04 - 3.14	45.	40.5
3.14 - 2.45	132.	91.
2.45 - 1.91	154.	83.
1.91 - 1.49	229.	96.
1.49 - 1.16	182.	60.
1.16 - 0.90	153.	40.
0.90 - 0.702	181.	36.
0.702 - 0.546	175.	27.
0.546 - 0.331	220.	47.
0.331 - 0.201	238.	31.
0.201 - 0.122	273.	22.
0.122 - 0.0449	693.	53.
Total		648.83

3. Gamma Radiation

3.1 Source Term

External gamma radiation in Pu-238 arises from three main sources:

1.) Prompt fission gammas (from spontaneous fission)

2.) Fission product gammas

3.) Decay of by-product isotopes of plutonium (mainly ^{236}Pu and its daughters)

Because the average half-life of the fission-products is short compared to the spontaneous fission half-life (4.9×10^{10} yr), the first two sources reach a steady state within a day after purification of the fuel. These are shown in Tables III and IV.

Table III. Prompt Fission Gammas From ^{238}Pu [4]

Energy Range	γ / gm-sec.
0.0 - 1.0	4650
1.0 - 3.0	1700
3.0 - 5.0	150
5.0 - 7.0	25

Table IV. Fission-Product Gamma Rays From ^{238}Pu [4]

Energy Range	γ / gm -sec.
0.1 - 1.0	5900
0.9 - 1.8	1000
1.8 - 3.0	450

^{236}Pu, an unwanted by-product of ^{238}Pu production, decays in a lengthy chain over a period of many years (Figure 2). This contributes a gamma ray source which increases in time, peaking some 18 years after purification (Figure 3). Table V shows the contribution to the source term of the three most significant gamma rays as a function of time.

Table V. Growth of Most Abundant ^{236}Pu Daughter Activity [4]
(1.2 ppm ^{236}Pu Initial Concentration)

Time after Purification (yrs.)	^{212}Pb 0.239 MeV (γ/ gm-sec)	^{208}Tl 0.583 + 2.62 MeV (γ / gm-sec)
0.1	330	260
1.0	27,000	21,000
2.0	90,000	70,000
5.0	330,000	260,000
10.0	570,000	450,000
18.0 (max.)	660,000	510,000

3.2 External Radiation

Table VI shows the calculated gamma spectrum at a detector point located at one-meter and 90-degrees from the axis of an MHW-RTG. Values for five year old fuel are given, based on an initial concentration of 1.2 ppm ^{236}Pu.

Clearly, a heat source in another geometric arrangement and surrounded by insulation instead of a thermoelectric generator will require a specific calculation for more exact data. Nevertheless the data presented in Tables II and VI should be adequate for an initial evaluation of the effects of neutron and gamma radiation on spacecraft equipment.

Figure 2 [5]

DECAY SCHEME OF ^{236}Pu

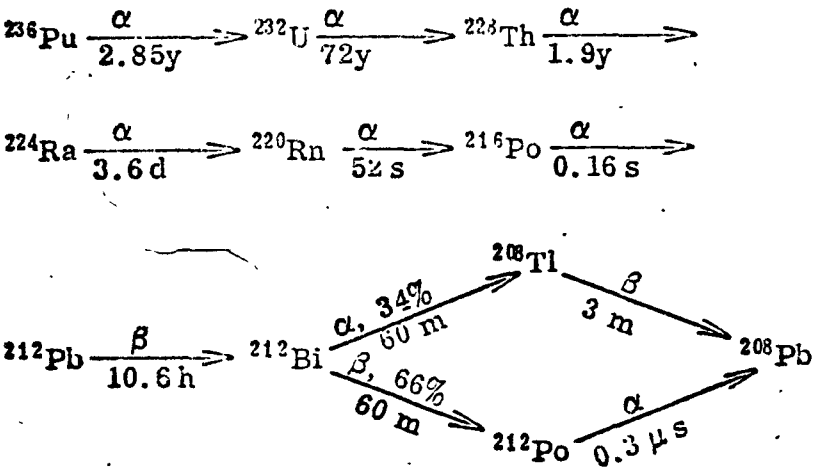

PRINCIPAL γ RADIATION

Element	γ-Energy	Abundance
^{212}Pb	0.24 Mev	82%
^{212}Bi	0.73 Mev	6%
^{208}Tl	0.58 Mev	30%
	2.6 Mev	34%

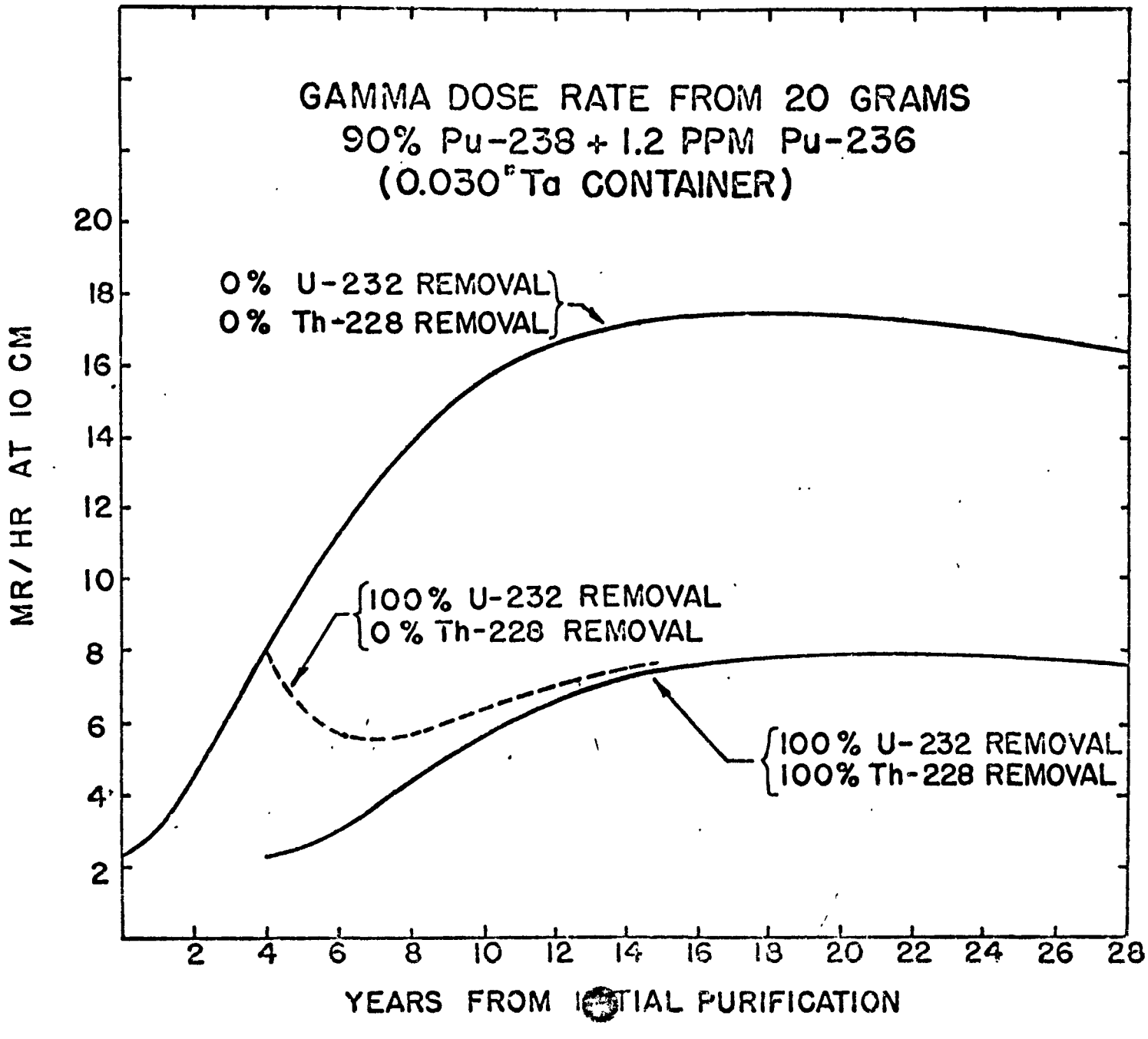
GAMMA DOSE RATE FROM 20 GRAMS
90% Pu-238 + 1.2 PPM Pu-236
(0.030" Ta CONTAINER)
MR/HR AT 10 CM
YEARS FROM INITIAL PURIFICATION
0% U-232 REMOVAL
0% Th-228 REMOVAL
100% U-232 REMOVAL
0% Th-228 REMOVAL
100% U-232 REMOVAL
100% Th-228 REMOVAL
2
4
6
8
10
12
14
16
18
20
22
24
26
28

Figure 3 [5]

Table VI. MHW-RTG Gamma Ray Spectrum [3]

at 1 meter, 90°

Group No.	Energy MeV	5-yr old fuel* No. Flux γ/cm^2-sec	Energy Flux Mev/cm^2-sec
1	7-6	7.28-2	4.73-1
2	6-5	2.16-1	1.19+0
3	5-4	6.41-1	2.88+0
4	4-3	1.85+0	6.47+0
5	3-2,616	1.70+0	4.77+0
6	2.616-2.614	8.94+2	2.34+1
7	2.614-2.0	1.75+2	4.04+2
8	2.0-1.75	1.17+2	2.19+2
9	1.75-1.50	1.16+2	1.88+2
10	1.50-1.25	1.02+2	1.40+2
11	1.25-1.0	1.51+2	1.70+2
12	1.0-.75	7.81+2	6.83+2
13	.75-.585	4.02+2	2.68+2
14	.585-.584	1.31+2	7.65+1
15	.584-.50	3.20+2	1.73+2
16	.50-.40	3.43+2	1.54+2
17	.40-.35	1.75+2	6.56+1
18	.35-.30	1.58+2	5.13+1
19	.30-.275	6.88+1	1.98+1
20	.275-.239	9.04+1	2.32+1
21	.239-.238	1.45+1	3.46+0
22	.238-.200	1.14+2	2.50+1
23	.200-.175	6.60+1	1.24+1
24	.175-.153	4.24+1	6.95+0
25	.153-.152	2.92+1	4.45+1
26	.152-.125	8.95+1	1.24+1
27	.125-.100	3.13+1	3.52+0
Totals		4.93+3	
Min Error:		3.02-2	
Mod Error:		7.03-2	
Max Error:		1.22-1	

* Initial concentration ^{236}Pu = 1.2 ppm; no Ir outer can

4. Measured Dose Rates

Recent measurements of the F-3 (flight unit) MHW Heat Source Assembly (HSA) for radiological survey purposes were conducted by Mound Laboratory personnel following encapsulation of the heat source. These results are reproduced below:

External radiation dose rates associated with HSA F-3 were measured from the surface of the source to the center of the detector, with the exception of the SPC configuration, whereby the dose rates were measured from the center of the source to the center of the detector. Gamma readings were taken with a Victoreen Radector III, and neutron readings were taken with an Eberline PNC-1.

HSA (During the Leak Check in the Passbox of Box 605)

Distance	mrem/hr γ	mrem/hr N^{o}	mrem/hr Total
23 cm (9")	15	252	267
32 cm (12")	10	180	190
62 cm (24")	4	100	104
91 cm (36")	2	36	38

HSA Inside the SPC

Distance	mrem/hr γ	mrem/hr N^{o}	mrem/hr Total
32 cm (12")	40	244	284
62 cm (24")	12	124	136
91 cm (36")	5	60	65

HSA in the Shipping Container

Distance	mrem/hr γ	mrem/hr N^{o}	mrem/hr Total
Surface of Wire Cage	.7	154	161
91cm(36") from Wire Cage	1	24	25
Surface of Shipping Container Lid	1.5	84	83.5

(SPC - Special Protective Container)

5. References

1. Data Sheets for PPO Radioisotope Fuel, Los Alamos Informal Report LA-5160-MS-Rev. 1 (Dec. 1973)
2. TOPS Final Report, RTG Radiation Analysis, Jet Propulsion Laboratory, 900-524 (April 1972)
3. Personal Communication, V. Truscello, Jet Propulsion Laboratory, (Feb. 1975)
4. Radiation Characteristics of Plutonium-238, G.M. Matlack, C.F. Metz, Los Alamos Scientific Laboratory, LA-3696 (October 1967)
5. Some Radiation Properties of Plutonium-238 Materials, Los Alamos Scientific Laboratory, Presented at NASA Ames Laboratory (May 7, 1970)

APPENDIX C

Heat Source Thermal Analysis

A three-dimensional thermal analysis of the reference heat source was performed. This analysis used an 18 degree symmetry argument about the cylinder longitudinal axis. The resultant segment was further divided by three planes as shown in Figure C-1. Each plane was systematically sub-divided into areas as shown in Figure C-2. The nodes used to develop the thermal network are located roughly at the centroid of the volume bounded by the planes previously described.

TAP-4, the modified version of the North American-developed Thermal Analyzer Program TAP-3, was used to solve for the nodal temperatures. TAP-4 is a finite difference code which can also be used to predict the heat source temperature distribution during both the fire and reentry transient. Materials properties data were filed as tables to accommodate the variations which occur along the gradients. The anistropy of Thornel and Pyrocarb were modeled.

The computer model was exercised for six different conditions of operation. These cases are outlined in the matrix shown in Table C-1.

Table C-1

Case	1	2	3	4	5	6
	Normal	Shutdown	Failure 1	Failure 2	Energy Dump	He leak
Refrigerator	on	off	off	off	off	on
Insulation	on	off	on	on	off	on
Coolant	on	on	on	off	off	on
He in Capsule Gaps	yes	yes	yes	yes	yes	no

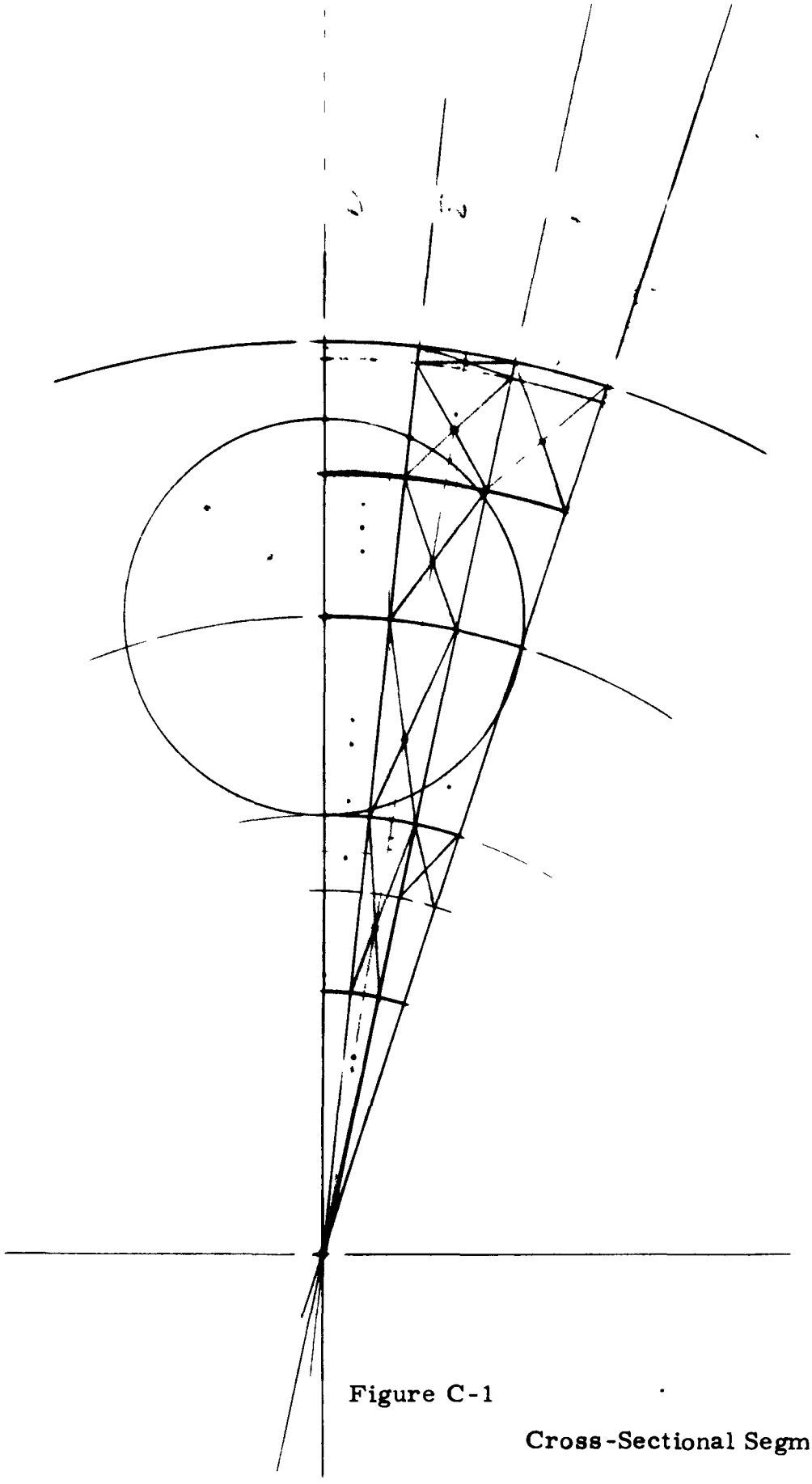

Figure C-1

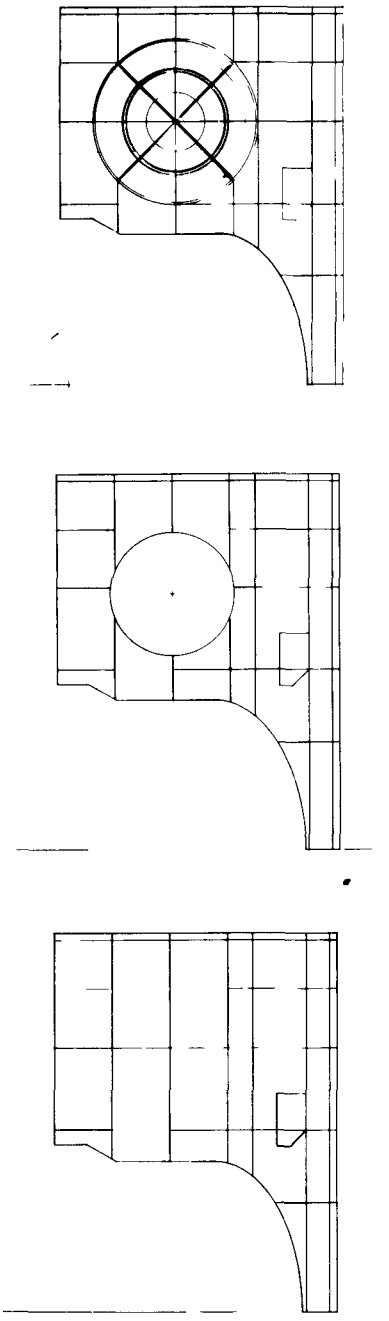

Figure C-2

Cross-Sectional Segments

Three hundred fifty temperatures were obtained for each case. The most pertinent of these are shown in Table C-2. A key to the location of the temperatures shown in Table C-2 is given in Figure C-3.

Table C-2

Temperature in Degrees Fahrenheit

Case	1	2	3*	4*	5	6
Location						
A	139	540	310	365	543	138
B	141	557	355	389	561	141
C	1490	640	3101	3291	645	1497
D	1454	650	3110	3304	655	1454
E	1560	631	3108	3295	635	1561
F	1580	671	3117	3312	677	1580
G	1523	715	3133	3326	720	1523
H	1610	741	3171	3349	747	1613
I	1720	849	3232	3421	778	2103
J	1880	943	3400	3589	950	2527
K	1550	711	3168	3330	717	1548
L	390	309	1836	2357	359	389
M	104	159	193	500	264	104
N	100	100	100	1131	218	100
O	135	562	312	318	567	115
P	1580	632	3110	3297	637	1565

* The results of cases 3 and 4 are unrealistic because no account of the melting of the nickel foil insulation was made. These cases were structured to show that sufficient driving force is available to melt the prescribed insulation and this will limit the system peak temperatures. Other methods of limiting the peak temperatures are also under analysis.

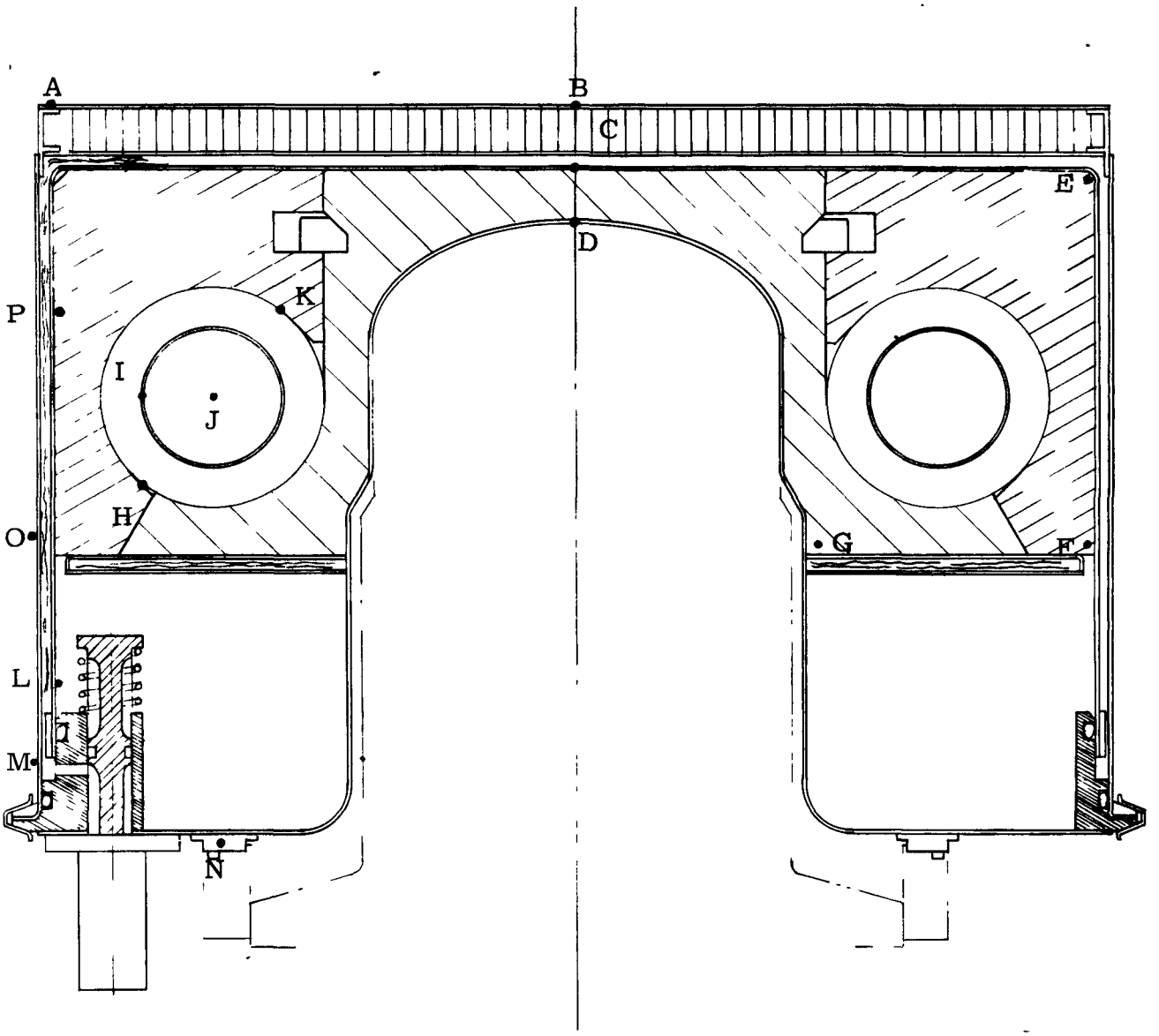

Figure C-3

Temperature Nodes Reported in Table C-2

APPENDIX D

Heat Source Heat Exchanger Description

The heat source exchanger (HSHX) (Figure 3) is fabricated from three sheets of .032" thick 6061 aluminum alloy, each approximately equivalent in size and shape to the developed surface area of the cylindrical heat source assembly (HSA). One sheet is corrugated over its surface except around the perimeter which is flat and coincides with the median plane of the sheet. The corrugated sheet forms the center element of a sandwich panel with the remaining two sheets as surface elements of the panel. The dimensional treatment of the three sheets along the long edges (which become the circumferencial ends of the cylinder) form integral headers on each side of the center sheet. The panel is assembled by positioning the three sheets into concentric cylinders, bonding the three sheets together in the corrugated area only using adhesives (having high peel and tensile strength and exhibiting compatibility with the cooling fluids used) and by welding the three sheets together along their periphery. Suitable fittings are attached to the headers for entrance and exit of the coolant.

The design provides two completely isolated coolant flow systems having a supply header encircling one end of the cylinder, a collector header similarly configured at the opposite end of the shroud, and a single longitudinal flow pass of the fluid between the headers through 126 identical passageways.

Fluid flow in the passageways is laminar; in the headers, fluid flow is part laminar and may be part turbulent. Pressure drop in the heat exchanger is calculated to be about 7 psi with the loss concentrated in the headers. Since the transition between laminar and turbulent flow may vary widely, depending on many factors, the head loss due to friction is also quite variable and is normally established by test. Because fluid flow rate is low, modest increases in header size produce significant reductions in fluid velocity and thereby, head loss; hence, head loss is considered to be no particular problem.

Coolant, upon entering the supply header, divides into two equal streams flowing around the toroidal header in opposite directions. The fluid disperses into the 126 longitudinal passages, recombines in the collector header and flows toward the exit port, again in two opposing paths. Table C-1 lists the design and operational characteristics of the heat exchanger shroud.

System design advantages

- The heat exchanger design has no "hidden" joints through which fluid could leak to another system. If small leaks occur through the adhesive bond joints, it is into an adjacent passageway of the same system. External seams are welded. Thus, the design may be produced, tested and repaired if leaks exist.
- The heat exchanger accommodates two independent coolant fluid systems. One system is used for orbital (spacecraft) operation. The second system is part of an auxilliary cooling system for operation during those times that heat cannot be satisfactorily dissipated by the spacecraft radiator, i.e., during launch or while enclosed in the Space Shuttle payload bay. The auxilliary system may be mounted in the Shuttle and connected to the spacecraft through two fluid lines using self-sealing quick disconnect fluid couplings.
- Valves are not required in the cooling fluid system for heat source thermal control. Coolant flow through refrigerator and heat source shroud are in series.
- Redundant pumps may be placed in the system in parallel by using a pressure actuated check valve in the output line of each pump to prevent reverse flow.

System Design Calculations

Table D-2 lists significant equations used in the design of the heat exchanger and Table D-3 gives the nomenclature for these design equations. Table D-4 presents physical characteristics of the coolant, Coolanol 15.

Equation 1 is the rate of energy reception by a flowing fluid. Equation 2 is the total convection heat transfer rate for a heat exchange surface that is tubular in shape. Δt_l is assumed constant throughout the length of the heat exchanger fluid passageways. Equation 3 is a correlation of heat transfer in laminar flow and is used in equation 2 as modified in equation 6 to obtain the temperature difference between the fluid and the walls.

Equation 4 presents a combination of those factors of the fluid evaluated at the mean temperature between inlet and outlet; the factor Γ_m is plotted in Figure D-1 as a function of the mean temperature of the fluid. Figures D-2 and D-3 permit rapid solution of equation 6 to establish the wall temperatures. NOTE: the design of the heat exchanger has assumed that the heat transferred to the fluid during passage through the headers is negligible. This is not strictly true and will be considered in detail final design of the heat exchanger.

Equation 7 through 10 identify friction factors and head loss associated with fluid flowing through enclosed channels and are used to establish the head loss in passing through the heat exchanger.

Equations 11, 12, and 13 are used in computing the temperatures of the surface of the heat source for given temperatures of the heat exchanger surface. The equation considers the area factors of the two surfaces and their proximity to each other. Equation 14 defines the heat flow into and out of the spacecraft external radiator.

Table D-1

Heat Exchanger Shroud Design Data

Type: Radiant energy input, and fluid cooled by conduction

Configuration: Cylindrical Shroud - 16" diameter, $8\frac{1}{2}$" long, two totally separated fluid compartments throughout shroud surface area, each capable of cooling the shroud.

Material: 6061 - T6 Al. Al.

Weight: Structure ≈5 lbs., Fluid ≈2.4 lbs.

Surface Coatings : Vapor deposited Kapton, e = .80

Fluid Path Characteristics

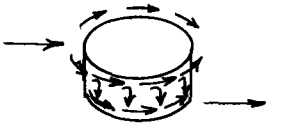

- Flow path ⟶
- Flow rate: 2.2 gpm
- Fluid, Spacecraft orbital operation: Coolanol 15
- Fluid, Auxilliary operation: TBD -- Nominally water.
- Number of longitudinal passageways: 126

Temperature, design condition, orbit system:

Fluid average temperature, t_m: (t in + t out)/ 2 = 20°C

Fluid temperature rise, Δt: 5.85°C

Shroud wall temperature, t_w: ≈ 42°C

Temperature design conditions, auxilliary cooler system using water:

Fluid coverage temp, t_m: 20°C

Fluid temperature rise: Δt = 2.5°C

Shroud wall temperature, t_w: ≈ 26°C

Table D-2

Correlation of heat transfer in laminar flow, in a tube, from Sieder & Tate (1963)

$$q = m c_p \Delta t \tag{1}$$

$$q = h_m \pi D L \Delta t_\ell \tag{2}$$

$$\frac{hD}{k_m} = 1.86 \left[\frac{DV}{\mathcal{V}_m}\right]^{\frac{1}{3}} \left[\frac{c_p \mu}{K}\right]_m^{\frac{1}{3}} \left[\frac{D_e}{L}\right]^{\frac{1}{3}} \left[\frac{\mu_m}{\mu_w}\right]^{0.14} \tag{3}$$

Solve for h and collect terms evaluated at t_m,

$$h_m = \left[1.86\, k_m \left(\frac{1}{\mathcal{V}}\right)_m^{\frac{1}{3}} \left(\frac{c_p \mu}{K}\right)_m^{\frac{1}{3}} \left(\mu\right)_m^{0.14}\right] \left(\frac{V}{D_e L}\right)^{\frac{1}{3}} \left(\frac{1}{\mu_w}\right)^{0.14}$$

$$\text{Let } \Gamma_m = \left[1.86\, K \left(\frac{1}{\mathcal{V}}\right)^{\frac{1}{3}} \left(\frac{c_p \mu}{K}\right)^{\frac{1}{3}} \left(\mu\right)^{0.14}\right]_m \tag{4}$$

$$\text{then } h_m = \Gamma_m \left(\frac{V}{D_e L}\right)^{\frac{1}{3}} \left(\mu_w\right)^{-0.14} \tag{5}$$

Substitute Eq (5) into Eq. (2) and rearranging terms gives

$$\left(\mu_w\right)^{-0.14} \Delta t_\ell = q / \left(\Gamma_m\right) \left(V D_e^2 L^2\right)^{\frac{1}{3}} \pi \tag{6}$$

$$F = \frac{4 f L V^2}{2 g_o D} \tag{7}$$

$$F = 0.00140 + 0.125 \left(\mu / DG\right)^{\frac{1}{3}} \quad \text{for turbulent flow in smooth tubes, from Koo, (1933)} \tag{8}$$

$$F = 64/N_R \quad \text{for streamline flow} \tag{9}$$

Δp = Fp Total Pressure Drop for Tube of Length L wherein "F" is valid (10)

$$q = A F_A F_\epsilon \sigma (T_1^4 - T_2^4) \quad (11)$$

$$F_\epsilon = \frac{1}{1/\epsilon_1 + (A_1/A_2)(1/\epsilon_2 - 1)} \quad \text{(For concentric spheres)} \quad (12)$$

$$F_A = 1 \quad \text{(For concentric spheres)} \quad (13)$$

$$q = \sigma \epsilon T^4 A_{TOTAL} - K_s \alpha A_{PROJ.} \quad (14)$$

Table D-3

Nomenclature for Design Equations

A = Area, sq. cm (subscript 1 refers to enclosed body, Eq. 11, 12)

D = Diameter, cm

D_e = Equivalent diameter = $4 H_R = 4 \frac{A}{P1}$

E_b = Total emissive power, Kg-cal/(m^2) (hr) $(^oK)^4$

f = Fanning friction factor

F = Friction loss, gm cm/gm of fluid passing

F_A = Area Factor

F_ϵ = Emissivity Factor

g_o = 980 gm cm/gm sec^2

G = $V\rho$ = mass velocity, gm/(sec) (cm^2)

H_R = Hydraulic Radius = A / P_1, cm

L = Length, cm

k = Thermal conductivity, cal/(^oC) (cm) (sec)

K = Solar Flux = 440 BTU/(HR) (ft^2)

m = Rate of mass flow gm/sec.

N_{Re} = Reynold's Number = $D_e V/$

$p_1 p_2$ = Pressure at inlet and outlet, respectively, gm/sq cm

P_1 = Wetted perimeter of the fluid passage, cm

q = Power, cal/sec

T = Absolute temp, ^oK

t_m = Mean temperature of fluid between inlet and outlet, ^oC

t_w = Temperature of wall at liquid interface, ^oC

V = Velocity, cm/sec

w = Weight rate of flow, gm/sec

Z = Distance measured in direction of flow, cm

Δt = Fluid temperature rise = t out = t in, ^oC

Δt_1 = Temperature difference between wall and fluid, ^oC

Δ_p = Pressure drop due to friction, bm/cm^2

c_p = Specific heat, cal/(gm) (^oC)

ϵ = Emissivity (non-dimensional) (Subscript 1 refers to enclosed body)

Table D-3 (cont)

μ = Absolute viscosity, = VP, gm/(cm) (sec)

ν = Kinematic viscosity, cm^2/sec = stokes

ρ = Density, gms/cm^3

σ = Stefan-Boltzmann constant = 4.88×10^{-8} kg-cal/(m^2) (hr) (^oK)^4

= 0.1714×10^{-8} Btu/ft^2) (hr) (^oR)^4

Table D-4

COOLANOL 15

T °F	T °C	K $\frac{cal}{(cm^2)(sec)\frac{^oC}{cm}}$	C_p $\frac{(cal)}{(gm)(^oC)}$	$\frac{cm^2}{sec}$ (stoke)	ρ $\frac{gm}{cm^3}$	μ $\frac{gm}{(cm)(sec)}$
-76	-60	29.7E-5	(.373)	.28	.956	.268
-58	-50	29.3E-5	(.380)	.17	.948	.161
-40	-40	29.1E-5	(.387)	.085	.939	.0798
-22	-30	28.7E-5	(.394)	.060	.931	.0559
-4	-20	28.4E-5	.401	.047	.922	.0433
14	-10	28.1E-5	.410	.037	.914	.0338
32	0	27.6E-5	.417	.030	.905	.0272
50	10	27.3E-5	.424	.024	.897	.0215
68	20	26.9E-5	.431	.0197	.888	.0175
86	30	26.5E-5	.438	.0168	.880	.0148
104	40	26.2E-5	.445	.0155	.872	.0135
122	50	25.8E-5	.452	.0130	.863	.0112
140	60	25.3E-5	.460	.0116	.855	.00992
158	70	24.8E-5	.467	.0108	.847	.00915
176	80	24.5E-5	.474	.0097	.838	.00813
194	90	23.9E-5	.481	.0089	.830	.00737
212	100	23.5E-5	.488	.0082	.821	.00673
230	110			.0075	.813	.00610

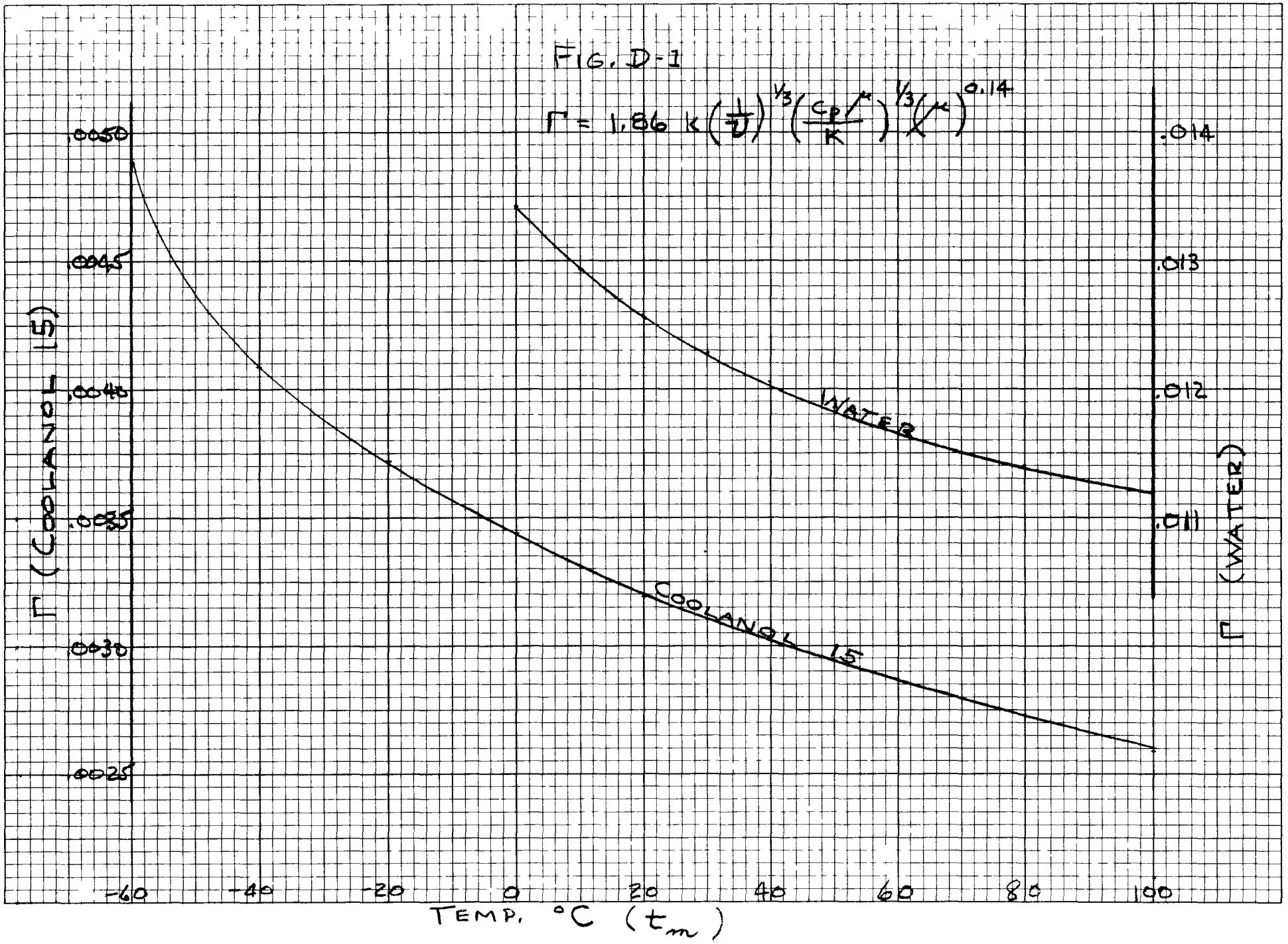
FIG. D-1
$\Gamma = 1.86\, k \left(\frac{1}{\nu}\right)^{1/3} \left(\frac{c_p \rho}{K}\right)^{1/3} \left(\frac{\rho}{\mu}\right)^{0.14}$
Γ (COOLANOL 15)
Γ (WATER)
.0050
.0045
.0040
.0035
.0030
.0025
.014
.013
.012
.011
WATER
COOLANOL 15
-60
-40
-20
0
20
40
60
80
100
TEMP. °C (t_m)

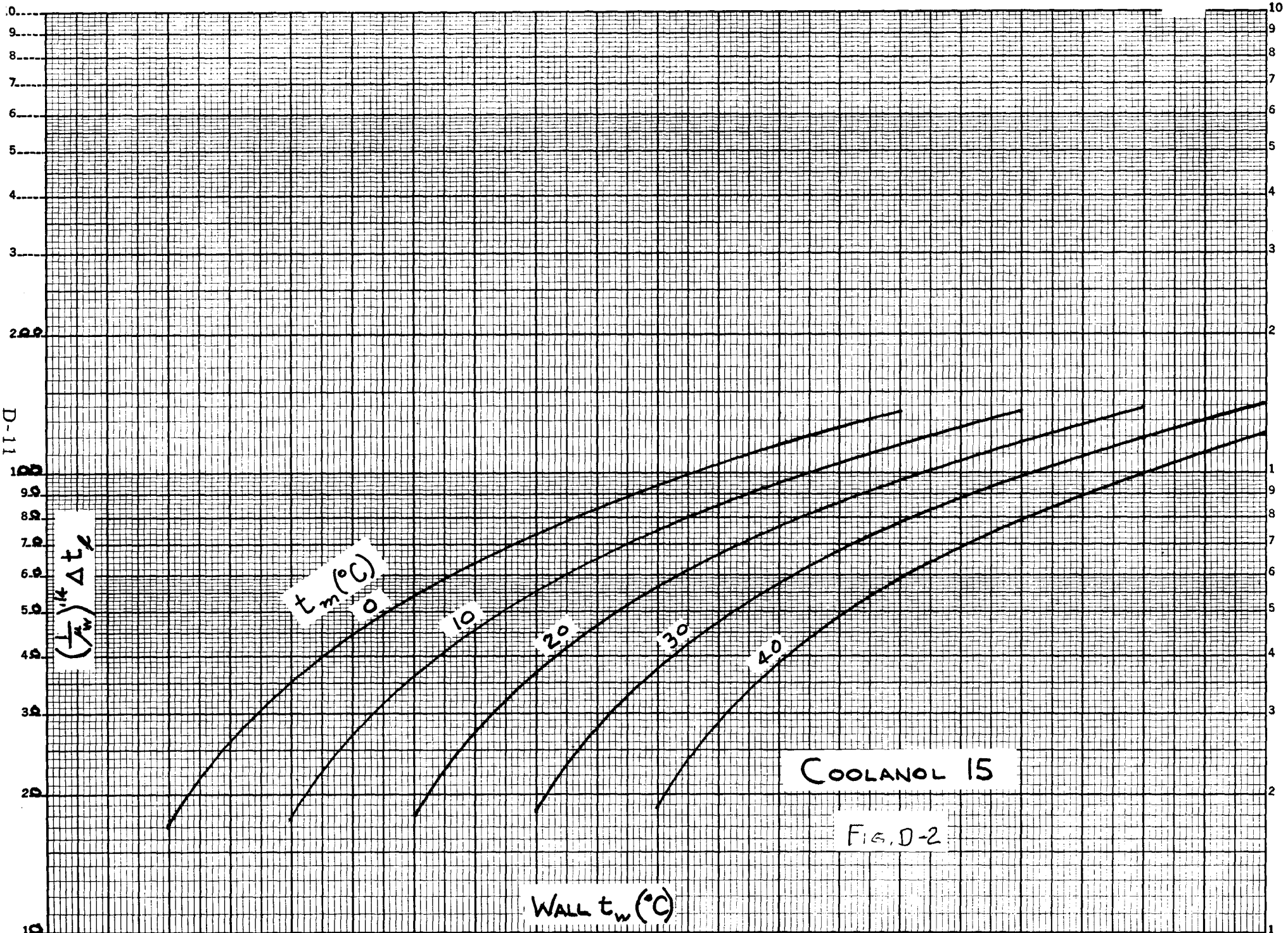
$\left(\frac{1}{\mu_w}\right)^{1/4} \Delta t_e$
t_m (°C)
0
10
20
30
40
COOLANOL 15
FIG. D-2
WALL t_w (°C)
10
20
30
40
50
60
70
80
90
100

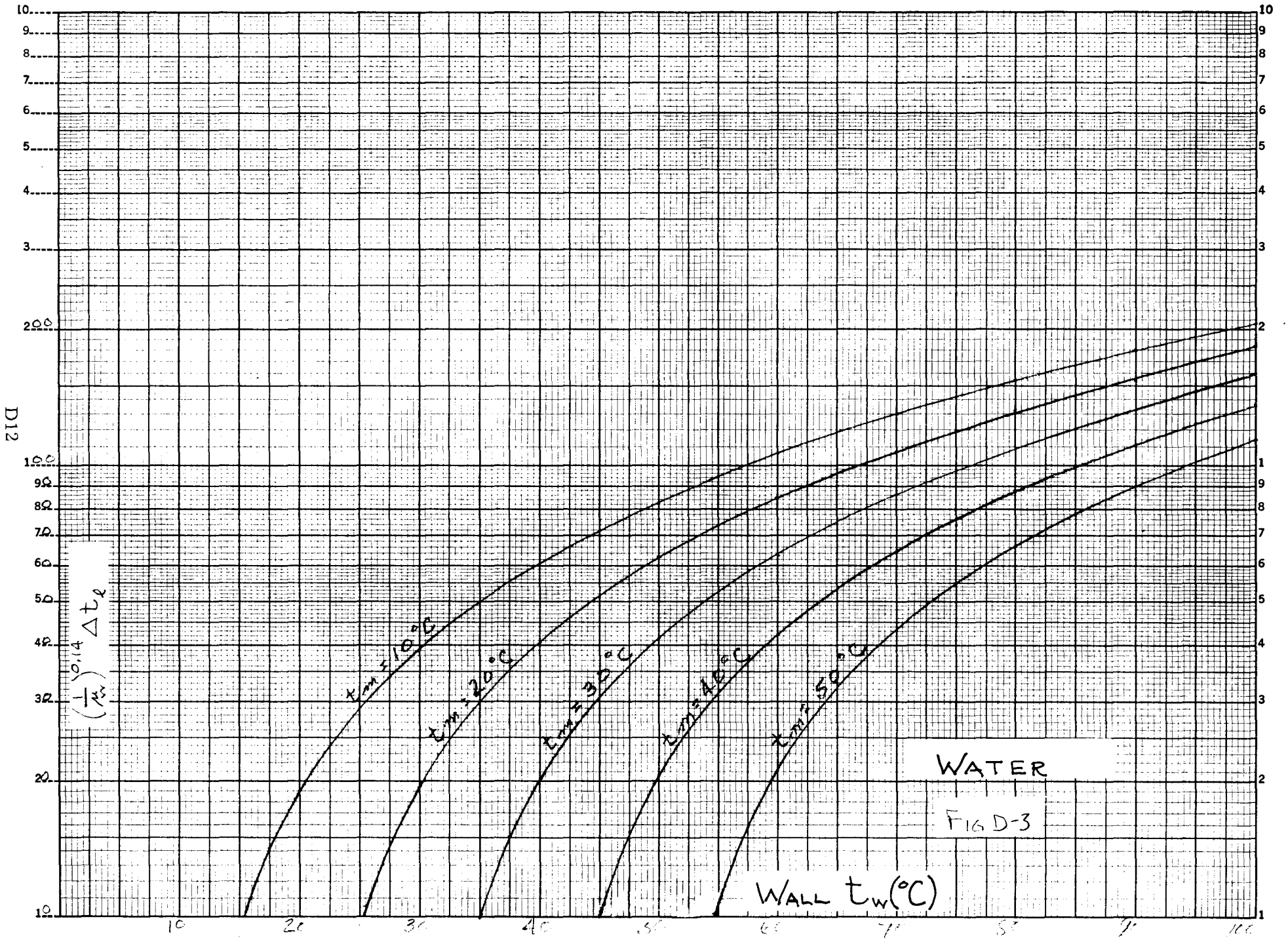
$\left(\frac{1}{\mu_w}\right)^{0.14} \Delta t_l$
$x_m = 10\,^\circ C$
$x_m = 20\,^\circ C$
$x_m = 30\,^\circ C$
$x_m = 40\,^\circ C$
$x_m = 50\,^\circ C$
WATER
FIG D-3
WALL t_w(°C)

References

Sieder, E.N., and G.E. Tate: Ind. Eng. Chem., vol. 28, p. 1429, (1936)

Drew, Koo, and McAdams: Trans. Am. Inst. Chem. Engrs., vol. 28, p.56. (1933).

Perry, J.H., Chemical Engineers Handbook. (1950)

Gebhart, B., Heat Transfer, McGraw-Hill Book Co. (1961)